

Review

# The Yin and Yang of Heartbeats: Magnesium–Calcium Antagonism Is Essential for Cardiac Excitation–Contraction Coupling

Chiara Marabelli <sup>1,2,3,\*</sup> , Demetrio J. Santiago <sup>3</sup>  and Silvia G. Priori <sup>1,2,3</sup>

<sup>1</sup> Department of Molecular Medicine, University of Pavia, 27100 Pavia, Italy

<sup>2</sup> Laboratory of Molecular Cardiology, IRCCS ICS Maugeri, 27100 Pavia, Italy

<sup>3</sup> Centro Nacional de Investigaciones Cardiovasculares Carlos III (CNIC), 28029 Madrid, Spain; demetriojulian.santiago@cnic.es

\* Correspondence: chiara.marabelli02@universitadipavia.it

## Abstract

While calcium ( $\text{Ca}^{2+}$ ) is a universal cellular messenger, the ionic properties of magnesium ( $\text{Mg}^{2+}$ ) make it less suited for rapid signaling and more for structural integrity. Still, besides being a passive player,  $\text{Mg}^{2+}$  is the only active  $\text{Ca}^{2+}$  antagonist, essential for tuning the efficacy of  $\text{Ca}^{2+}$ -dependent cardiac excitation–contraction coupling (ECC) and for ensuring cardiac function robustness and stability. This review aims to provide a comprehensive framework to link the structural and molecular mechanisms of  $\text{Mg}^{2+}/\text{Ca}^{2+}$  antagonistic binding across key proteins of the cardiac ECC machinery to their physiopathological relevance. The pervasive “dampening” effect of  $\text{Mg}^{2+}$  on ECC activity is exerted across various players and mechanisms, and lies in the ions’ physiological competition for multiple, flexible binding protein motifs across multiple compartments.  $\text{Mg}^{2+}$  profoundly modulates the cardiac action potential waveform by inhibiting the L-type  $\text{Ca}^{2+}$  channel Cav1.2, i.e., the key trigger of cardiac ryanodine receptor (RyR2) opening. Cytosolic  $\text{Mg}^{2+}$  favors RyR2 closed or inactive conformations not only through physical binding at specific sites, but also indirectly through modulation of RyR2 phosphorylation by Camk2d and PKA. RyR2 is also potently inhibited by luminal  $\text{Mg}^{2+}$ , a vital mechanism in the cardiac setting for preventing excessive  $\text{Ca}^{2+}$  release during diastole. This mechanism, able to distinguish between  $\text{Ca}^{2+}$  and  $\text{Mg}^{2+}$ , is mediated by luminal partners Calsequestrin 2 (CASQ2) and Triadin (TRDN). In addition,  $\text{Mg}^{2+}$  favors a rearrangement of the RyR2 cluster configuration that is associated with lower  $\text{Ca}^{2+}$  spark frequencies.



Academic Editor: Michael X. Zhu

Received: 7 July 2025

Revised: 7 August 2025

Accepted: 14 August 2025

Published: 18 August 2025

**Citation:** Marabelli, C.; Santiago, D.J.; Priori, S.G. The Yin and Yang of Heartbeats: Magnesium–Calcium Antagonism Is Essential for Cardiac Excitation–Contraction Coupling. *Cells* **2025**, *14*, 1280. <https://doi.org/10.3390/cells14161280>

**Copyright:** © 2025 by the authors. Licensee MDPI, Basel, Switzerland. This article is an open access article distributed under the terms and conditions of the Creative Commons Attribution (CC BY) license (<https://creativecommons.org/licenses/by/4.0/>).

## 1. Introduction

The role of calcium ( $\text{Ca}^{2+}$ ) as a universal second messenger cannot be overstated.  $\text{Ca}^{2+}$  is omnipresent, involved in processes spanning from the shortest time scales (e.g., vesicular fusion in the  $\mu\text{s}$  range) to the years-long occurrence of diseases (e.g., heart failure) [1,2]. Cells go to great lengths in order to contain, store, and profit from the signaling actions of  $\text{Ca}^{2+}$ :  $\text{Ca}^{2+}$  buffers serve as contention means, organelles such as the sarco-endoplasmic reticulum and mitochondria serve as  $\text{Ca}^{2+}$  storage areas, and  $\text{Ca}^{2+}$ -sensing proteins are used for local and global signaling [1,3,4]. Hormones carefully regulate extracellular  $\text{Ca}^{2+}$  levels in the larger organismal context.

The above mechanisms, however, only contextualize and address the signaling actions of  $\text{Ca}^{2+}$ , without truly tuning it. It is magnesium ( $\text{Mg}^{2+}$ ), a relatively similar cation in appearance, that allows modulation of the amplitude of  $\text{Ca}^{2+}$ -dependent processes by antagonizing them. By opposing and competing with each other,  $\text{Ca}^{2+}$  and  $\text{Mg}^{2+}$  successfully defeat dangerous increases in cellular entropy [4–8].

This review focuses on the roles played by  $\text{Mg}^{2+}$  in cardiac excitation–contraction coupling (ECC), a  $\text{Ca}^{2+}$ -controlled process by which the heartbeat occurs in the millisecond time scale. We will start by discussing the ionic nature of  $\text{Mg}^{2+}$  as compared to  $\text{Ca}^{2+}$ , and how their differences are employed by biological systems to elicit distinct and antagonistic mechanisms. We will further explore the structural characteristics of  $\text{Ca}^{2+}$ - and  $\text{Mg}^{2+}$ -binding sites in different cardiac proteins, and dissect how the most delicate  $\text{Ca}^{2+}$ -dependent ECC mechanisms are also sensitive to  $\text{Mg}^{2+}$ . In between, we will briefly touch upon those  $\text{Mg}^{2+}$ -related aspects that concern heart pathophysiology. The organismal and cellular regulations of  $\text{Mg}^{2+}$  levels are outside the scope of this review: the reader is referred to [9,10] for excellent discussions. By examining the intricate interplay between  $\text{Mg}^{2+}$  and  $\text{Ca}^{2+}$  in cardiac EC coupling, this review seeks to provide a comprehensive understanding of  $\text{Mg}^{2+}$ 's crucial modulatory role, from its molecular binding sites and their selectivity to its profound clinical implications.

## 2. The Basis of the Antagonistic Actions by $\text{Ca}^{2+}$ and $\text{Mg}^{2+}$

$\text{Mg}^{2+}$  is the second most abundant intracellular cation in cardiomyocytes, with a total concentration about 10 mM [11], of which the free  $\text{Mg}^{2+}$  concentration is tightly maintained in the 0.5 to 1 mM range [1,5,12–14]. Exactly because of the very small fluctuations in free  $\text{Mg}^{2+}$  abundance, studies on cellular dynamic processes have mainly focused on the orders of magnitude larger variation in  $\text{Ca}^{2+}$  concentrations, largely obscuring the  $\text{Mg}^{2+}$ -dependent fine adjustments of these same processes, including cardiac homeostasis [10,15]. Despite both being divalent cations, fundamental differences in their ionic properties shape their distinct, often competitive, interactions with various proteins. The  $\text{Ca}^{2+}$  ion features a larger ionic radius (1.05 Å) than that of  $\text{Mg}^{2+}$  (0.78 Å). This implies a lower charge density and consequently a lower desolvation energy. Together with the easier exchange of ligand partners, the variable coordination number of  $\text{Ca}^{2+}$  (between 6 and 9) allows it to be easily grabbed by solvent-exposed protein motifs within geometrically flexible coordination complexes [16]. In contrast, free  $\text{Mg}^{2+}$  is usually present within a stable hydration shell, shaped by the rigid octahedral disposition of six water molecules, the removal of which is energetically very demanding [16,17]. In addition, it is not unusual for this ion to have additional water layers around it, so that changes of up to 400 times in volume have been reported between hydrated and non-hydrated  $\text{Mg}^{2+}$ , compared to a ~25-fold difference for  $\text{Ca}^{2+}$  [18,19]. This increase in radius, unlike calcium, prevents magnesium from passing through narrow ion channels. Indeed, few  $\text{Mg}^{2+}$  transporters are known.

The above differences between  $\text{Ca}^{2+}$  and  $\text{Mg}^{2+}$  dictate the structure of their protein binding sites and their functional effects in biological systems. The flexibility of  $\text{Ca}^{2+}$  coordination within proteins acquires a functional role in processes such as sarcomere contraction, opening of transmembrane channels, and activation of signaling enzymes.  $\text{Ca}^{2+}$  binding occurs at flexible and adaptable protein motifs, such as the EF-hand motif (found in cardiac troponin C (cTnC) and calmodulin (CaM)), and is coordinated by mixed ligand types (e.g., aspartate, glutamate, asparagine, and carbonyl oxygens) [16,20,21].

On the other hand, the tight coordination of  $\text{Mg}^{2+}$  atoms is usually shaped by the octahedral disposition of six hard oxygens from carboxyl groups (Asp, Glu) and/or phosphates (ATP, GTP, etc.), with a lower variability in the distances between cation and oxygen atom compared to  $\text{Ca}^{2+}$  (2.05 to 2.25 Å for  $\text{Mg}^{2+}$  vs. 2.2 to 2.7 Å for  $\text{Ca}^{2+}$ ) [19]. The energetically

expensive and structurally rigid binding of  $Mg^{2+}$  is better suited for the structural integrity of proteins (this implication is supported by 40% more proteins containing  $Mg^{2+}$  vs.  $Ca^{2+}$  atoms, as published in the RCSB Protein Data Bank [22]).  $Mg^{2+}$  is also a structural cofactor for ATP-dependent enzymes like kinases and ATPases, whereby it facilitates catalysis by stabilizing transition states or providing a binding site for substrates.

However, the distinction between the architectures of protein  $Ca^{2+}$ - and/or  $Mg^{2+}$ -binding sites is not strictly binary. Many protein sites bind both cations, sometimes even in the same buffer condition [21,23]. The ground of the competition between  $Mg^{2+}$  and  $Ca^{2+}$  ions occurs exactly within this spectrum of protein divalent-binding sites, mainly at the larger and more flexible motifs rather than at the rigid and smaller ones evolutionarily designed for  $Mg^{2+}$  binding. In addition to the binding site design, the protein dynamics and the ionic environment also shape the relative binding equilibria of  $Mg^{2+}$  and  $Ca^{2+}$ . The functional implication is that  $Mg^{2+}$ , whose intracellular concentration oscillates far less than that of  $Ca^{2+}$ , acts as a natural competitive “damping agent” of  $Ca^{2+}$ -dependent events. When transient spikes of  $Ca^{2+}$  occur,  $Mg^{2+}$  is displaced and  $Ca^{2+}$ -dependent signaling mechanisms are unlocked.

### 3. $Ca^{2+}$ -Driven ECC Runs Across Multiple Cellular Landscapes

Cardiac ECC is the fundamental  $Ca^{2+}$ -dependent process by which an electrical stimulus, the action potential (AP), is translated into coordinated contraction of the myocardial cells. As finely tuned,  $Ca^{2+}$ -dependent interconnections between sequential stages occurs in distinct cellular compartments, not only the dynamics of  $Ca^{2+}$ -handling proteins, but also their precise spatial arrangement, are extremely critical to ECC [1,24].

#### 3.1. Structural Aspects of Cardiac ECC

ECC occurs in specialized structures within myocytes known as “dyads”, formed by periodically or near-periodically juxtaposed areas of the sarcolemma or its invaginations, the transverse (T-) tubules, and highly specialized domains of the sarcoplasmic reticulum known as the “junctional” sarcoplasmic reticulum (jSR). The juxtaposition of both organelles forms a narrow ( $\leq 20$  nm) [25], protein-rich, and diffusionaly constrained environment known as the “dyadic space”. Certain proteins, such as Junctophilin 2 (JPH2), are capable of structurally linking the two organelles by dwelling within both membranes simultaneously.

#### 3.2. Functional Aspects of Cardiac ECC

ECC is initiated by the arrival of an AP at the dyadic sarcolemma (i.e., by a rapid, transient change in the voltage across the membrane). This electrical signal triggers the opening of voltage-sensitive, transmembrane L-type  $Ca^{2+}$  channels (Cav1.2) [24,26], causing a minor influx of extracellular  $Ca^{2+}$  into the narrow dyadic space. Here, due to diffusional constriction [25], a few  $Ca^{2+}$  ions can translate into relatively high concentrations and rapidly activate clusters of jSR-embedded,  $Ca^{2+}$ -sensitive  $Ca^{2+}$  release channels (known as ryanodine receptors type 2; RyR2s) [13,27,28]. This cytosolic  $Ca^{2+}$ -dependent RyR2 activation, known as cell-wide  $Ca^{2+}$ -induced  $Ca^{2+}$  release (CICR), leads to a substantial outflow of  $Ca^{2+}$  through the RyR2 channels from the jSR lumen into the cytosol [24,27,29], which is in turn used for cellular contraction plus other regulatory pathways (depending on heart rate, metabolic demands, pathophysiological status, etc.). The cytosolic  $Ca^{2+}$  concentration rises from a diastolic (resting if cell not stimulated) 100 nM value to peaks of 1  $\mu M$  during systole [1].

CICR does occur stochastically and locally at low frequency in cells (the so-called “ $Ca^{2+}$  sparks”), which occurs when the statistically improbable openings of nearby Cav1.2s

and/or RyR2s synchronize and the influx of  $\text{Ca}^{2+}$  towards the dyadic space triggers the opening of neighboring RyR2s.

$\text{Mg}^{2+}$  acts as an inhibitor of this CICR process, both by competitive inhibition of  $\text{Ca}^{2+}$ -dependent activation sites and by inhibiting RyR2 by itself at  $\text{Ca}^{2+}/\text{Mg}^{2+}$ -dependent inactivation sites [30] (see below sections). To understand the relevance of  $\text{Mg}^{2+}$  inhibition to CICR in physiological conditions, it must be pointed out that, out of the (up to) 100 RyR2s present in a murine RyR2 cluster, on average only 9–11 RyR2s activate at the peak of a murine  $\text{Ca}^{2+}$  spark [31]. Besides the effects of  $\text{Mg}^{2+}$ , additional mechanisms further regulate the likeliness of CICR in major ways, such as RyR2 fragmentation into subclusters [32], the presence/absence/mutation of Junctophilin 2 [33], dyadic buffering [34], and free levels of jSR  $\text{Ca}^{2+}$  [35].

In the presence of a cardiac AP, depolarization opens many Cav1.2s, the  $\text{Ca}^{2+}$  stimulus becomes persistent,  $\text{Mg}^{2+}$  is displaced by  $\text{Ca}^{2+}$  at the RyR2  $\text{Ca}^{2+}$ -dependent activation site, and  $\text{Ca}^{2+}$  sparks synchronize to produce the whole-cell  $\text{Ca}^{2+}$  transient. In certain pathophysiological states (e.g., hypomagnesemia, arrhythmias, heart failure, SR  $\text{Ca}^{2+}$  overload), or when the sarcolemma is damaged, untimely  $\text{Ca}^{2+}$  release may occur in the absence of an AP. Such CICR is sequential and fueled by a “fire–diffuse–fire” mechanism:  $\text{Ca}^{2+}$  is spontaneously released from existing dyads, and it diffuses and triggers CICR at nearby dyads without Cav1.2 involvement. This “fire–diffuse–fire” also occurs physiologically during systole in instances where the association between T-tubules and jSR is not present (e.g., at the center of atrial cells and iPSC-derived cardiomyocytes) or has been lost (failing ventricular myocytes), the latter at the cost of cardiac output [36].

For completeness, we must add that ECC comprises two signaling pathways: anterograde Cav1.2-to-RyR2 signaling, which leads to CICR (discussed above); and retrograde RyR2-to-Cav1.2 signaling (via  $\text{Ca}^{2+}$  release), which leads to Cav1.2  $\text{Ca}^{2+}$ -dependent inactivation. This retrograde pathway contributes to AP repolarization and prevents cells from overloading with  $\text{Ca}^{2+}$ .

Furthermore, the link between CICR, Cav1.2 inactivation, SERCA-mediated uptake, and NCX-mediated extrusion of cytosolic  $\text{Ca}^{2+}$  constitutes the basis of so-called “ $\text{Ca}^{2+}$  autoregulation”, which develops in time frameworks of several beats and homeostatically maintains cardiac output. Autoregulation also explains why  $\text{Ca}^{2+}$ -handling-dependent arrhythmias do not occur at baseline situations but instead occur during beta-adrenergic stimulation [37]. While the  $\text{Mg}^{2+}$ -dependent effects on the aforementioned pathways will be discussed below, we know of no studies specifically focused on the overall  $\text{Mg}^{2+}$  regulation of  $\text{Ca}^{2+}$  autoregulation, and therefore we will no longer focus on this aspect of ECC.

### 3.3. $\text{Mg}^{2+}$ Shapes the Kinetics of Contraction and Relaxation

During individual  $\text{Ca}^{2+}$  sparks, the amount of non-diffusible  $\text{Ca}^{2+}$ -binding partners between dyads and myofilaments is so large that it limits the increase in free  $\text{Ca}^{2+}$  to sub-micron distances from the release sites.  $\text{Ca}^{2+}$  diffusion is supported by ATP, a highly mobile and abundant (up to 5 mM in cardiac cells)  $\text{Ca}^{2+}$  buffer, with very fast on–off kinetics for both  $\text{Ca}^{2+}$  and  $\text{Mg}^{2+}$ . ATP avidly binds some of the released  $\text{Ca}^{2+}$  (therefore releasing  $\text{Mg}^{2+}$  bound during diastole) and facilitates the trip of complexed  $\text{Ca}^{2+}$  towards the contractile filaments [38]. Additionally, spatiotemporal summation of sparks during whole-cell ECC allows more  $\text{Ca}^{2+}$  to reach the myofilaments.

Once at the contractile elements and when in free form,  $\text{Ca}^{2+}$  binds to cardiac troponin C (cTnC). As cytosolic  $\text{Ca}^{2+}$  displaces  $\text{Mg}^{2+}$  in binding to cTnC, it induces a conformational change in the troponin–tropomyosin complex, which in turn exposes the actin–myosin binding sites and allows sarcomere contraction [21,39], which itself depends on Mg-ATP.

For relaxation to occur,  $\text{Ca}^{2+}$  is removed from the cytosol primarily by the Sarco/Endoplasmic Reticulum  $\text{Ca}^{2+}$ -ATPase (SERCA), which populates at high density the membrane of the non-junctional sarcoplasmic reticulum [24]. This  $\text{Ca}^{2+}$  removal mechanism, once again, depends on Mg-ATP expenditure. Secondly, the sodium–calcium exchanger (NCX), located in the sarcolemma (yet excluded from the immediate dyadic junctions), provides bulk  $\text{Ca}^{2+}$  extrusion from the cardiomyocyte into the extracellular space, in a  $\text{Mg}^{2+}$ -dependent manner (see below).

Lastly, as mentioned above, part of the released  $\text{Ca}^{2+}$  is used for non-ECC purposes. The mitochondrial calcium uniporter (MCU), generally lying in the outer mitochondrial membrane in very close proximity to the jSR, contributes to  $\text{Ca}^{2+}$  homeostasis while triggering intra-mitochondrial  $\text{Ca}^{2+}$ -signaling cascades for the stimulation of oxidative metabolism [1,15,40–42]. This jSR-mitochondrial coupling is important mechanistically, as it allows the heart to adjust to different heart rates. Notice that at increased heart rates,  $\text{Ca}^{2+}$  release occurs more often, so  $\text{Ca}^{2+}$  enters mitochondria more frequently and more ATP can be produced to match the increases in Mg-ATP expenditure for both the contraction and recycling of ions. That said,  $\text{Ca}^{2+}$  is only able to increase respiration by a factor of ~2, where changes in left ventricular filling can increase respiration more than 10-fold, so this ECC-related mechanism is still a small contributor to myocardial energetics [43].

#### 4. $\text{Mg}^{2+}/\text{Ca}^{2+}$ Crosstalk Across ECC Key Cytosolic Compartments

The vital competition between  $\text{Mg}^{2+}$  and  $\text{Ca}^{2+}$  during ECC occurs at distinct timings and spaces: the cytosol, the narrow dyadic space, and the jSR lumen. The concentration distribution of each ion across distinct cellular compartments, and the ion-binding properties and dynamics of the residing proteins, dictate the functional outcome of their crosstalk [1,24]. The overall ECC process thus relies on very subtle differences in  $\text{Ca}^{2+}$  and  $\text{Mg}^{2+}$  handling and signaling across compartments, up to the point that dysregulation of a single component in a single cellular location can affect the entire process.

In the cytosol, both during diastole/at rest and during contraction, the concentration of free  $\text{Mg}^{2+}$  (in the 0.8–1 mM range) is orders of magnitude higher than that of cytoplasmic  $\text{Ca}^{2+}$ , fluctuating from 100 nM to approximately 1  $\mu\text{M}$  during systole [1,10,24]. This vast numerical advantage endows  $\text{Mg}^{2+}$  with a large advantage in competing with  $\text{Ca}^{2+}$  at shared binding sites on various proteins [4,10,15]. More specifically,  $\text{Mg}^{2+}$  functionally antagonizes  $\text{Ca}^{2+}$  at sites critical for ionic channels [12,26,27]. In addition, a large portion (about 5 mM) of intracellular  $\text{Mg}^{2+}$  is retained through the binding of ATP [26,44,45]. The homeostasis of  $\text{Mg}^{2+}$  is indeed intimately linked to ATP levels: depletion of ATP, exacerbated by conditions such as alcohol exposure, can lead to impaired  $\text{Mg}^{2+}$  retention within mitochondria and the cytoplasm [46]. Conversely, this binding also ensures the availability of Mg-ATP, the physiologically active form of ATP [1,17,47].

##### 4.1. Effects on Cellular Excitability

The sarcolemma is equipped with a battery of ion channels and transporters that regulate the various ionic currents of the cardiac AP (Figure 1A). Despite being often neglected,  $\text{Mg}^{2+}$  profoundly modulates the AP waveform through its intricate interactions with sarcolemmal ion channels (Figure 1B), often through direct and specific mechanisms [15,48] but also through action on other protein interactors such as G-proteins [48]. In addition, extracellular  $\text{Mg}^{2+}$  and  $\text{Ca}^{2+}$  both screen the negative charges on the outside of the sarcolemma and channel proteins. This screening effect confers a proper voltage-dependent behavior to ion channels, affecting how they open and inactivate [49].

#### 4.1.1. Main Depolarizing (Inward) Currents

The sodium current ( $I_{Na}$ ) is mediated by voltage-gated  $\text{Na}^+$  channels (mainly Nav1.5), and is responsible for the rapid sarcolemmal depolarization (phase 0, Figure 1). Evidence in ventricular cells suggests  $\text{Mg}^{2+}$  primarily exerts an open-channel blocking effect on outward currents in a concentration- and voltage-dependent manner, with limited direct allosteric modulation [50]. The biological implications of such  $\text{Mg}^{2+}$ -dependent regulation, if any, remain unknown, as there is no outward  $I_{Na}$  in cardiac cells in physiological conditions.

The L-type  $\text{Ca}^{2+}$  current ( $I_{\text{CaL}}$ ), mediated by Cav1.2s, is the principal maintainer of the AP plateau (phase 2, Figure 1) and the provider of the trigger  $\text{Ca}^{2+}$  influx ( $I_{\text{CaL}}$ ) that initiates cardiac ECC. Its high sensitivity to intracellular  $\text{Mg}^{2+}$  concentration has been more deeply studied than that of many other channels, revealing that  $\text{Mg}^{2+}$  exerts both direct and indirect inhibitory effects [4,7,51]. Structural and mutagenesis studies indicate that  $\text{Mg}^{2+}$  binding to an EF-hand motif in the C-terminal domain of Cav1.2 reduces peak current amplitude and enhances voltage-dependent inactivation (VDI) [13,52,53]. During myocardial ischemia, where ATP hydrolysis leads to a rise in cytosolic  $\text{Mg}^{2+}$  to 2.1–2.3 mM [53,54],  $\text{Mg}^{2+}$ -dependent suppression of  $I_{\text{CaL}}$  shortens AP duration, mitigating both  $\text{Ca}^{2+}$  overload and cytotoxicity. Conversely, in pathological conditions like heart failure, low  $\text{Mg}^{2+}$  levels contribute to an adaptive increase in  $I_{\text{CaL}}$ , increasing the susceptibility to arrhythmias and impaired relaxation [52,54,55]. Moreover,  $\text{Mg}^{2+}$  antagonizes the  $\beta$ -adrenergic receptor ( $\beta$ -AR)-PKA pathway both by reducing the affinity of PKA for activating  $\text{Ca}^{2+}$  and by limiting the structural flexibility of the CaV1.2 cytoplasmic domain, hence the availability of exposed serines as substrates for PKA [8,13].

#### 4.1.2. Main Repolarizing (Outward) Currents

The effects of  $\text{Mg}^{2+}$  in the transient outward current ( $I_{\text{to}}$ ), which is responsible for the AP hump (phase 1, Figure 1), have not been widely studied in humans, where the current is mainly mediated by Kv4.3 channels, with some contribution by Kv4.2. In rats, where this current is mainly mediated by Kv4.2,  $\text{Mg}^{2+}$  deficiency was shown to produce a decrease in the levels of Kv4.2 mRNA and protein, leading to corresponding decreases in  $I_{\text{to}}$  [56].

Delayed rectifier  $\text{K}^+$  currents ( $I_{\text{Kr}}$ ,  $I_{\text{Ks}}$ ) are also critical repolarizing currents, defining the duration of the AP plateau (phase 2) and phase 3 (Figure 1).  $I_{\text{Kr}}$  studies in nominally  $\text{Mg}^{2+}$ -free intracellular solution suggest that  $\text{Mg}^{2+}$  does not block the pore of the HERG channel [57]. Additional studies suggest that intracellular  $\text{Mg}^{2+}$  above 10  $\mu\text{M}$  is needed to maintain repolarization reserve [58].

The inward rectifier  $\text{K}^+$  current ( $I_{\text{K1}}$ ), mediated by Kir2.1 channels, is fundamental for enabling rapid membrane repolarization during phase 3 of the AP and for maintaining a stable resting membrane potential during phase 4 (Figure 1). During the plateau of the cardiac AP (phase 2), the membrane potential is more positive on the inside of the sarcolemma than on its outside, creating a local driving force for  $\text{Mg}^{2+}$  ions towards the pore of open Kir2.1 channels. This  $\text{Mg}^{2+}$  binds the pore, leading to voltage-dependent open-channel block and causing a characteristic inward rectification (i.e., block of outward  $\text{K}^+$  currents at depolarized potentials) [4,7,48,59]. At membrane potentials progressively closer to the resting membrane potential (i.e., phases 3 and 4 of the AP),  $\text{Mg}^{2+}$  ions progressively abandon Kir2.1 pores, allowing a normal flow of  $\text{K}^+$  ions, which repolarizes the membrane and maintains the resting membrane potential.  $\text{Mg}^{2+}$  block is remarkably instantaneous, and involves the Ser165 and Asp172 residues in the transmembrane domain (TM2), whereas Glu224 and Glu299 at the cytoplasmic bundle-crossing region determine the  $\text{Mg}^{2+}$  sensitivity [59]. Experimentally, it has been shown that  $\text{Mg}^{2+}$  deficiency can cause transcriptional downregulation of the amounts of Kir2.1 mRNA and protein. Conversely,  $\text{Mg}^{2+}$  overload upregulates the amounts of Kir2.1 [56]. An in silico study specifically

analyzed the effects of hypomagnesemia on IK1 rectification while maintaining constant Kir2.1 levels and in the absence of hypomagnesemia-related changes to other ionic currents. The study concluded that a lack of Mg<sup>2+</sup> in these simulated conditions would unexpectedly decrease outward IK1 currents, leading to prolonged AP duration (see Figure 5 therein), which in turn could result in increased risk of arrhythmias (early afterdepolarizations, heterogeneity of AP duration) [60].

The Na<sup>+</sup>/K<sup>+</sup> ATPase current (INaK) maintains the resting membrane potential and repolarizes the AP (Figure 1B) [61]. Mg<sup>2+</sup> deficiency contributes to cardiac arrhythmia by disrupting the activity of this ATPase due to lower Mg-ATP levels [62].

#### 4.1.3. Other Repolarizing Currents

The muscarinic K<sup>+</sup> current (IK, ACh, Kir3.1) is predominantly found in atrial and nodal cells, controlling diastolic potential and pacemaker depolarization [48]. Similarly to IK1, the inward rectification of IK<sub>ACh</sub> is fundamentally due to a voltage-dependent block by internal Mg<sup>2+</sup>. However, the voltage-dependent sensitivity of this block differs significantly from that of IK1, implying unique Mg<sup>2+</sup>-binding site properties [7].

ATP-Sensitive K<sup>+</sup> (KATP, Kir6.2) currents link cellular metabolic state to excitability via a linear current–voltage dependency. As the Kd for Mg<sup>2+</sup> block is voltage-dependent, ranging from approximately 10 mM at −60 mV to 0.5 mM at +40 mV, Mg<sup>2+</sup>-dependent inhibitory effects are also voltage-dependent. In addition, MgADP binding activates the channel by counteracting Mg-ATP inhibition [7,48].

#### 4.1.4. Na<sup>+</sup>/Ca<sup>2+</sup> Exchange

The NCX-dependent current (INCX) can behave as either a depolarizing or a repolarizing current depending on the specific timing within the AP and ionic conditions. Early into the action potential, INCX brings a tiny amount of Ca<sup>2+</sup> inside cells, whereas during most of the AP and diastole it removes Ca<sup>2+</sup> from the cytosol. Despite this primary importance for cell relaxation and Ca<sup>2+</sup>, only a few studies have addressed the effects of intracellular Mg<sup>2+</sup> on INCX. NCX activity is strongly increased by intracellular calcium, at a specific intracellular allosteric regulatory site. The competition between Mg<sup>2+</sup> and Ca<sup>2+</sup> for binding to this site suggests that low Mg<sup>2+</sup> levels may promote arrhythmogenesis and cellular Ca<sup>2+</sup> loss (e.g., heart failure) via NCX dysregulation [6,48,63].

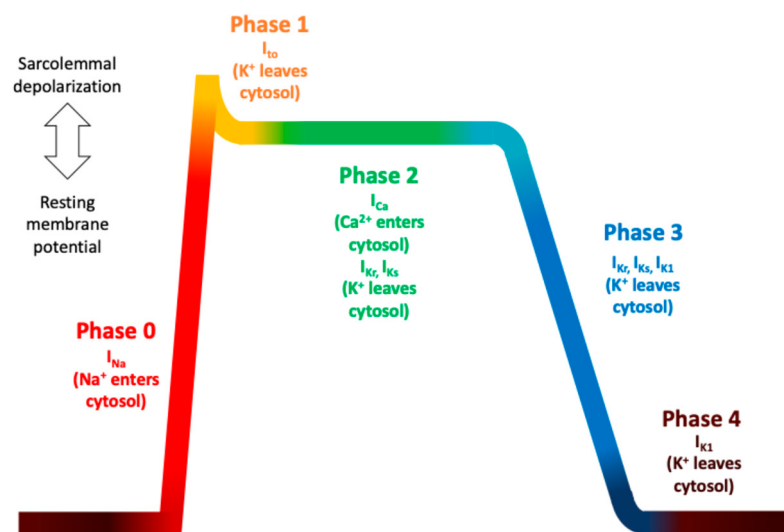
### 4.2. Effect on Cellular Contractile Response

In addition to its structural presence at sites III and IV of cardiac troponin C (cTnC), physiological amounts of Mg<sup>2+</sup> compete with Ca<sup>2+</sup> for binding at the regulatory site II of cTnC [21,64]. This specific interaction impacts the Ca<sup>2+</sup> sensitivity of every single myofilament and thus the contractile force generated by the overall muscle. In hypertrophic cardiomyopathy, mutations in cTnC alter the protein's affinity for both Ca<sup>2+</sup> and Mg<sup>2+</sup>, disrupting contractile regulation [21].

### 4.3. Effect on Relaxation

SERCA (more specifically SERCA2a in the cardiac muscle) is the workhorse of cardiac relaxation, actively pumping Ca<sup>2+</sup> from the cytosol back into the SR. Mg<sup>2+</sup> is essential for coordinating ATP during the phosphorylation step of the pump cycle [16,65]. Molecular dynamics simulations have shown that Mg<sup>2+</sup> can compete with Ca<sup>2+</sup> for binding to SERCA's canonical Ca<sup>2+</sup>-binding sites (sites I and II) [65]. Other effects of Mg<sup>2+</sup> on SERCA are expectedly mediated by the various Mg-ATP-dependent kinases, acetylases, and SUMOylases that control its activity and that of its main inhibitory partner, phospholamban (PLB) [66,67].

### (A) Main AP ionic currents



### (B) $[\text{Mg}^{2+}]_{\text{cytosol}}$ -dependent regulation

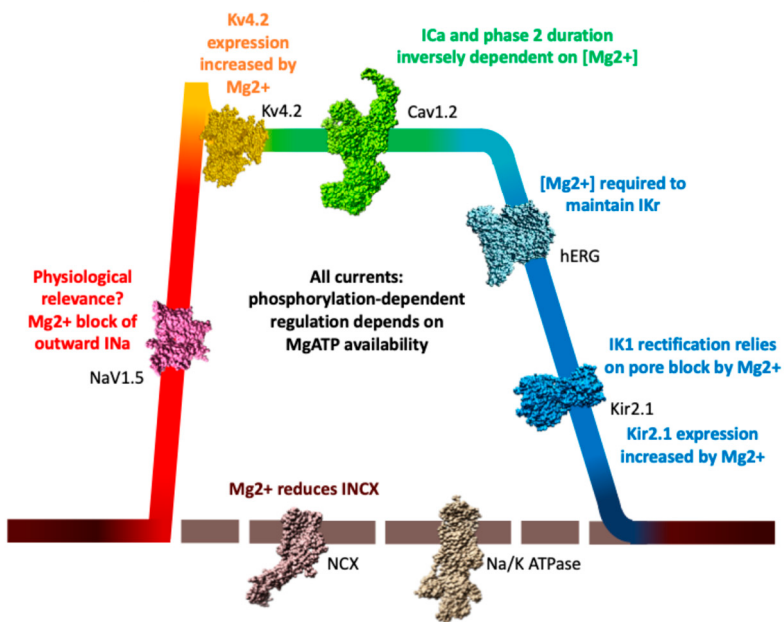


**Figure 1.**  $\text{Mg}^{2+}$ -sensitive ionic currents shaping the ventricular cardiomyocyte AP. (A) A schematic representation of the ventricular cardiomyocyte AP phases: phase 0 (rapid depolarization), phase 1 (initial repolarization), phase 2 (plateau), phase 3 (repolarization), and phase 4 (resting potential). The top-left white arrow symbolizes the status of the membrane potential during the different phases of the AP. (B) Ionic channels and transporters known to be modulated by  $\text{Mg}^{2+}$  and relevant to ventricular cardiomyocyte function are indicated here. These include the rapid depolarizing sodium current  $I_{Na}$  (Nav1.5, PDB ID: 7DTD [68]), transient outward potassium current  $I_{to}$  (Kv4.2, PDB ID: 7F0J [69]), L-type calcium current  $I_{CaL}$  (Cav1.2, PDB ID: 8WE6 [70]), delayed rectifier potassium currents  $I_{Kr}$  and  $I_{Ks}$  (here represented by channel hERG for  $I_{Kr}$ , PDB ID: 5VA1 [71]), inward rectifier potassium current  $IK1$  (Kir2.1, PDB ID: 7ZDZ [72]),  $\text{Na}^+/\text{Ca}^{2+}$  exchanger (NCX, PDB ID: 8JP0 [73]), and  $\text{Na}^+/\text{K}^+$  ATPase (PDB ID: 7E1Z [74]).  $\text{Mg}^{2+}$  modulates these targets through direct effects (such as pore block, voltage-dependent inhibition, or direct binding) or indirect effects (including altered channel expression, ATP availability for kinase activity), thereby influencing AP morphology, calcium cycling, and overall cardiac excitability.

## 5. The Core of CICR: Ryanodine Receptor Type 2 (RyR2)

RyR2 is the principal actor of the core mechanism of cardiac ECC, that is, CICR, a highly delicate process where even subtle defects can lead to severe cardiac pathologies, including arrhythmias and heart failure [27,75,76]. The tight coordination of events in CICR, and their extreme sensitivity to ionic variations, are supported by the precise juxtaposition in space of the protein machineries involved. Within the dyadic cleft, the principal voltage-dependent trigger, CaV1.2, lies within a dozen nanometers of the mouth of the RyR2 pore, so that small variations in  $\text{Ca}^{2+}$  abundance are rapidly perceived [25,77]. In addition, RyR2 responsiveness is also modulated from the highly  $\text{Ca}^{2+}$ -enriched jSR luminal side, where a highly specialized set of ion-sensitive interactors is located [1].

### 5.1. $\text{Mg}^{2+}$ 's Effect on the Ultrastructure of the Dyad

Within the junctional SR membrane, RyR2 clusters and superclusters form the structural basis for elementary  $\text{Ca}^{2+}$  release units that underlie ECC. These clusters exhibit distinct spatial arrangements, and  $\text{Mg}^{2+}$  concentration is a key determinant of their configuration [78,79]. Under high- $\text{Mg}^{2+}$  conditions, RyR2 tetramers preferentially adopt a side-by-side arrangement. In contrast, low  $\text{Mg}^{2+}$  promotes a checkerboard configuration [78]. Functionally, these structural differences have profound effects: while side-by-side arrangements (favored by high  $\text{Mg}^{2+}$ ) are associated with lower  $\text{Ca}^{2+}$  spark frequencies, the checkerboard arrangement (favored by low  $\text{Mg}^{2+}$ ) leads to markedly increased spark frequencies [78].

Beyond the above effects, Mg-ATP availability determines RyR2 phosphorylation status during  $\beta$ -adrenergic stimulation. Such phosphorylation not only decreases the inhibitory effect of cytosolic  $\text{Mg}^{2+}$  on RyR2s [80] (see below) but also recruits PKA-phosphorylated RyR2s to the vicinity of Cav1.2s [81].

Another key determinant of dyadic ultrastructure is Junctophilin 2 (JPH2), which by binding to both sarcolemmal and jSR membranes simultaneously ensures a proper geometric relationship between both structures, and hence proper ECC. JPH2 has been shown to interact with the lipid PtdIns(3,4,5)P3, and divalent cations ( $\text{Ca}^{2+}$  and  $\text{Mg}^{2+}$ ) above 0.25 mM were found to perturb this association [82]. It follows that, in physiological conditions (0.5–1 mM free  $\text{Mg}^{2+}$ ), the presence of  $\text{Mg}^{2+}$  ensures the proper association between the jSR and T-tubule. This JPH2-mediated role of  $\text{Mg}^{2+}$  structurally safeguards the efficacy of the ECC process, which relies on the very tight ultrastructure and geometries of the dyadic space.

### 5.2. Cytosolic Modulation of RyR2

On the cytoplasmic side, RyR2 exposes a massive, 28×28 nm large platform for interaction with numerous partners and cofactors, including the Mg-ATP necessary for channel activation [27,83,84]. Here, cytosolic  $\text{Mg}^{2+}$  modulates the RyR2 open probability through multiple direct and indirect mechanisms [54,85]. Because of the high functional interdependency among cytosolic sites, and between cytoplasmic and luminal divalent-dependent processes, the precise determination of the specific properties of each  $\text{Ca}^{2+}/\text{Mg}^{2+}$ -binding site is an intrinsically complex challenge.

It is well known that the RyR2 response to cytosolic  $\text{Ca}^{2+}$  is biphasic: micromolar  $\text{Ca}^{2+}$  levels activate RyR2 while millimolar  $\text{Ca}^{2+}$  levels inhibit the channel. Both these processes are targets of  $\text{Mg}^{2+}$  functional effects.  $\text{Mg}^{2+}$ -binding sites have been identified for skeletal RyR1 through single-particle cryo-EM experiments [84], whereas for the specific case of cardiac RyR2, no bound  $\text{Mg}^{2+}$  has been resolved. Therefore, to point out the relevant functional consequences of  $\text{Mg}^{2+}$  in cardiac ECC we will build not only on the multiple

functional experimental insights into RyR2, but also upon the structural homologies and differences of Mg<sup>2+</sup> binding to either cardiac or skeletal RyR.

### 5.2.1. The A-Site

The main inhibitory effect of cytosolic Mg<sup>2+</sup> on RyR2 derives from its binding to the high-affinity, activating A-site within the central domain and in proximity to the caffeine- and ATP-binding sites. The A-site mediates Ca<sup>2+</sup>-dependent activation with a typical Ca<sup>2+</sup>-affinity of approximately 1 μM, ten times the diastolic Ca<sup>2+</sup> concentration [12,85–88]. Despite the 50-fold selectivity for Ca<sup>2+</sup> over Mg<sup>2+</sup> [86], the typical cytosolic abundance of the latter shifts the Ka of this site for Ca<sup>2+</sup> up to 50 μM [26,89,90], effectively blocking spontaneous Ca<sup>2+</sup> release. Mutagenesis studies on RyR2 highlighted a possible cause of the different functional outcomes of A-site binding by either Ca<sup>2+</sup> or Mg<sup>2+</sup>. The inhibitory effect of Mg<sup>2+</sup> implies binding to a set of oxygen-containing residues that, while being relevant to the Ca<sup>2+</sup>-activation mechanism, are not directly involved in Ca<sup>2+</sup>-coordination [91,92]. Recent cryo-EM analysis of the homologous RyR1 A-site revealed a mechanism that reconciles both the incomplete superposition of the Ca<sup>2+</sup>- and Mg<sup>2+</sup>-binding set of residues with their functional competition: steric fitting of a partially hydrated Mg<sup>2+</sup> ion, while increasing the solvent exposure of the A-site compared to the closed state, does not cause the large cavity expansion observed in presence of Ca<sup>2+</sup> (Figure 2) [84]. Mg<sup>2+</sup> stabilizes an inactive yet “dormant” state, still accessible to Ca<sup>2+</sup> and thus “primed” for rapid Ca<sup>2+</sup>-induced activation.

### 5.2.2. The I1-Site

The inhibitory I1-site is non-selective for Ca<sup>2+</sup> vs. Mg<sup>2+</sup>, and mediates channel closure at millimolar quantities of cytosolic divalent ions [86]. The skeletal muscle isoform features a much higher sensitivity to Mg<sup>2+</sup> vs. RyR2 (with IC50 values of 0.1 vs. 2–6 mM, respectively, Table 1), which makes it very unlikely that, in physiological settings, cytosolic Mg<sup>2+</sup> triggers significant RyR2 inhibition in the heart [12,27,84,85]. However, it is tempting to observe that, given the functional intertwining among multiple sites that is typical of RyRs, this minor divalent-inhibitory site may acquire a functional relevance in more pathological scenarios, such as hypermagnesemia, or during cellular Ca<sup>2+</sup> overload. Because of the lack of published Mg<sup>2+</sup>-bound RyR2 structures, we will here rely on structural-functional studies on the skeletal isoform, RyR1, to offer interesting clues on the presumed topology of I1-sites in RyR2. Mutagenesis and structural studies on RyR1 identified two putative locations featuring the expected I1-site properties (low-affinity and non-specific divalent cation binding), where Mg<sup>2+</sup> acts as a surrogate for Ca<sup>2+</sup> in stabilizing the closed state [84,93]. The first putative location for the I1-site corresponds to a diffuse electrostatic surface on the junctional solenoid (Jsol) domain (Figure 2), which is a key structural lever mechanically connecting the conformational rearrangements of the cytoplasmic regulatory domains to the pore gating machinery [94]. The fact that RyR1 features a distinctive sequence of 30 negative amino acids in this region (not present in RyR2), may explain the different sensitivities to divalent cations between the two isoforms. The second putative location, the EF-hand domain, is conserved between RyR1 and RyR2, and shares the same functional characteristics. In response to the low-affinity binding of both Ca<sup>2+</sup> and Mg<sup>2+</sup>, the EF-hand of RyR1 forms salt bridges with a neighboring subunit and stabilizes the closed conformation of the channel. As the EF-hand domains of the skeletal and cardiac isoforms share similar binding affinities, it was proposed that the higher efficiency of Cav1.1-RyR1 signal transmission in skeletal muscle ECC may functionally offset the higher RyR1 sensitivity to Mg<sup>2+</sup> inhibition [93].

**Table 1.** A summary of known  $\text{Ca}^{2+}$  and  $\text{Mg}^{2+}$  binding sites in ryanodine receptor isoforms. The table lists binding sites for  $\text{Ca}^{2+}$  and  $\text{Mg}^{2+}$  identified in ryanodine receptor type 1 (RyR1, skeletal muscle) and type 2 (RyR2, cardiac muscle). For each site, the structural location, known coordinating residues, relative affinity for  $\text{Mg}^{2+}$  versus  $\text{Ca}^{2+}$ , and functional outcomes of  $\text{Mg}^{2+}$  binding are summarized. Sites include the high-affinity cytosolic activation site (A-site), inhibitory sites (I1 and I2), the EF-hand/S2-S3 loop interface, the Jsol (handle) domain, ATP-binding sites, the selectivity filter, and luminal sites. Where available, structural data supporting  $\text{Mg}^{2+}$  coordination are indicated. For RyR2,  $\text{Mg}^{2+}$  binding has often been inferred based on homologous sites resolved in RyR1 structures. References on the structural location of the functional sites have been categorized as follows: <sup>a</sup>: based on homology with RyR1, for which structural evidence is reported; <sup>b</sup>: based on mutagenesis or trypsinization studies; <sup>c</sup>: based on rational or computational hypotheses.  $P_o$ : open probability.

Side	Site	Protein Location	Ion Binding Properties	Functional Consequence of $\text{Mg}^{2+}$
Cytosolic	A-site	Within central domain, in proximity to C-terminal domain and to ATP-binding site [84] <sup>a</sup> , [91] <sup>b</sup>	$K_a$ for $\text{Ca}^{2+}$ = 2–5 $\mu\text{M}$ $K_a$ for $\text{Mg}^{2+}$ = 50 $\mu\text{M}$ [12, 86, 93, 95, 96]	$\text{Mg}^{2+}$ shifts the apparent $K_a$ for $\text{Ca}^{2+}$ up to 50 $\mu\text{M}$ [86] and stabilizes an inactive state yet accessible to $\text{Ca}^{2+}$ [84].
	I1-site	Two putative locations: I. Electrostatic surface of Jsol domain [97] <sup>c</sup> II. Interface between EF-hand and S2-S3 loop [84] <sup>a</sup> , [93] <sup>c</sup>	RyR2 $IC_{50}$ $\text{Mg}^{2+}$ = 2–10 mM RyR1 $IC_{50}$ $\text{Mg}^{2+}$ = 0.1 mM [12, 27, 84, 85]	$\text{Mg}^{2+}$ acts as a surrogate for $\text{Ca}^{2+}$ in stabilizing the closed state. Physiological cytosolic $\text{Mg}^{2+}$ is unlikely to trigger an inhibitory mechanism through the I1-site in cardiac muscle.
	I2-site	Estimated at a 26 nm distance from the cytosolic channel mouth; possibly identifies with an inhibitory, $\text{Ca}^{2+}$ -sensing protein interactor [98]	RyR2 $K_a$ for $\text{Ca}^{2+}$ = 1 $\mu\text{M}$ [98]	$\text{Mg}^{2+}$ produces partial inactivation (20–40% reduction in open probability) in response to high levels of $\text{Ca}^{2+}$ “feed-through” from the jSR. Physiological $\text{Mg}^{2+}$ is largely unlikely to impact RyR2.
	ATP-Binding Pocket	Cavity between the central domains (U-motif and S6) and the C-terminal domain [84] <sup>a</sup>	$EC_{50}$ for Mg-ATP = 0.2 mM [99]	Binding of Mg-ATP induces a “primed” state, more susceptible to $\text{Ca}^{2+}$ -induced activation. Mg-ATP is essential for the luminal partner CASQ2 to inhibit RyR2 channel activity.
Transmembrane	Pore	In RyR1: D4945 (corresponding to D4875 in RyR2) lining the pore in S6 helices [54] <sup>c</sup> , [84] <sup>a</sup>	RyR1: Selective for stable $\text{Mg}^{2+}$ binding over $\text{Ca}^{2+}$ [84]	RyR1: $\text{Mg}^{2+}$ stabilizes the closed state, increasing resistance to pore opening [84]. RyR2: $\text{Mg}^{2+}$ at this site is not described. The RyR2 channel is permeable to $\text{Mg}^{2+}$ just as it is to $\text{Ca}^{2+}$ [54].
	Selectivity Filter	Conserved GGGIG motif within the S5–S6 loop (residues 4790–4830 in human RyR2) [54, 84] <sup>c</sup>	RyR1 and RyR2: Higher charge density expectedly favors $\text{Mg}^{2+}$ binding over $\text{Ca}^{2+}$ [54] RyR1 $IC_{50}$ $\text{Eu}^{3+}$ = 0.4 mM at 100 nM $[\text{Ca}^{2+}]_{\text{cyt}}$ [100].	There is expected similarity with the biphasic effect of $\text{Ca}^{2+}$ and $\text{Eu}^{3+}$ on RyR2, activating at submicromolar concentrations and inhibiting at higher than 1 $\mu\text{M}$ concentrations [100].
	Intrinsic Luminal Activation site	Proposed within intraluminal S1-S2 EF-hand motif [98] <sup>b</sup> , [100, 101] <sup>c</sup> , and proximal to S6-helical bundle [102] <sup>b</sup>	RyR2 $EC_{50}$ $\text{Ca}^{2+}/\text{Mg}^{2+}$ = 0.2–0.5 mM [103]	During pathological SR overload, when the inhibitory interaction with partners is lowered, maximal open probability is enhanced by luminal $\text{Ca}^{2+}/\text{Mg}^{2+}$ ions.
Luminal	Intrinsic Luminal Inhibition site	Proposed close to channel activation gate, near RyR1 Q4933 [100, 101] <sup>c</sup>	RyR2 $P_o$ inhibited by 15 $\mu\text{M}$ luminal $\text{Eu}^{3+}$ at 100 nM $[\text{Ca}^{2+}]_{\text{cyt}}$ [100]	Unknown.
	CASQ2-dependent Inhibitory L-site	Proposed binding of CASQ2 at RyR2-specific S1-S2 EF-hand [104] <sup>b</sup> Proposed binding of TRDN at S3-S4 loop [105, 106] <sup>b</sup>	Voltage-independent $K_a$ for $\text{Ca}^{2+}/\text{Mg}^{2+}$ = 35–45 $\mu\text{M}$ at 100 $\mu\text{M}$ luminal $\text{Ca}^{2+}$ [98] Hill coefficient = 2	At physiological concentrations, luminal $\text{Mg}^{2+}$ shifts the $K_a$ for luminal $\text{Ca}^{2+}$ activation to 1 mM.

### 5.2.3. The I2-Site

Differently from the I1-site, which is more functionally relevant for the skeletal RyR1, the I2-site was primarily described in RyR2. It is a cytosolic site with micromolar affinity for  $\text{Ca}^{2+}$ , able to produce a partial inactivation (20–40% reduction in the open probability) in response to high levels of  $\text{Ca}^{2+}$  feed-through from the jSR [98]. While a precise identification of the residues comprising the I2-site is missing,  $\text{Ca}^{2+}$ -diffusion/buffering experiments estimated that the I2-site is so much further away from the channel mouth (about 26 nm) that it may identify with an inhibitory  $\text{Ca}^{2+}$ -sensing protein interactor [98]. The specific functional relevance of these I2-site-mediated inhibition processes in the context of cellular RyR2 function is not yet clear, likely because of the stronger and masking effect of  $\text{Mg}^{2+}$  inhibition at the A-site [86].

### 5.2.4. The Channel Pore

In RyR1, robust structural data shows that  $\text{Mg}^{2+}$  binds directly within the pore (notably Asp4945, Figure 2), tightening the S6 helical bundle and increasing the resistance to pore opening [84]. MD experiments confirmed that this coordination, occurring exclusively in the closed state, is selective for  $\text{Mg}^{2+}$  over  $\text{Ca}^{2+}$  [93]. Since these structural insights on  $\text{Mg}^{2+}$ -coordination at the pore functionally belong to the low-affinity cytosolic  $\text{Mg}^{2+}$  inhibition mechanism in RyR1, and considering the high sequence homology between RyR2 and RyR1 in the pore-forming region [107], it is reasonable to infer that a comparable direct pore occlusion mechanism could exist in RyR2 yet be far weaker. What is known with certainty is that RyR2 is permeable to  $\text{Mg}^{2+}$  just as it is to  $\text{Ca}^{2+}$ , so that, under resting conditions, the expectedly symmetric distribution of  $\text{Mg}^{2+}$  across the SR membrane renders RyR2 a functionally  $\text{Mg}^{2+}$ -selective pore in terms of occupancy. Even though net current flow remains  $\text{Ca}^{2+}$ -selective, the presence of  $\text{Mg}^{2+}$  halves it [54]. In addition, the presence of  $\text{Mg}^{2+}$  in the pore directly points to the so-called “feed-through” effect of luminal  $\text{Mg}^{2+}$ , theoretically able to reach the cytosolic A-site and thus inhibit RyR2. However, as the variation in  $\text{Mg}^{2+}$  may be lower than 1 mM, the extent of such an effect may be strongly limited [27]. In failing hearts or catecholaminergic polymorphic ventricular tachycardia (CPVT), RyR2 sensitivity to  $\text{Mg}^{2+}$  inhibition is decreased, promoting arrhythmogenic  $\text{Ca}^{2+}$  release [76,83].

### 5.2.5. The ATP-Binding Pocket

In addition to the aforementioned divalent cation binding sites, it has to be considered that cytosolic  $\text{Mg}^{2+}$  also permits the binding of ATP, in the Mg-ATP complex form, within the cavity between central domains and the C-terminal domain (Figure 2). However, the different allosteric dynamics of RyR1 and RyR2 lead to distinct outcomes: while the presence of Mg-ATP is dispensable in RyR1 for  $\text{Ca}^{2+}$ -independent channel opening, in RyR2 it rather induces a “primed” state, making the channel more susceptible to  $\text{Ca}^{2+}$ -induced activation [83]. ATP activation of both RyR1 and RyR2 has an EC<sub>50</sub> in the range of 0.3–1 mM (Table 1). Given the physiological abundance of 5 mM Mg-ATP in cardiac cells, its maximal effect on RyR1/2 is always exerted [2]. Of note, it has been shown that presence of Mg-ATP on the cytosolic side of RyR2 is essential for the luminal partner CASQ2 to inhibit the RyR2 channel [108].

### 5.2.6. The $\text{Ca}^{2+}/\text{Mg}^{2+}$ -Sensitive Cytosolic Interactome of RyR2

The uniquely large cytosolic portion of the RyR2 tetramer also allows for interactions with a wealth of protein partners and enzymes. Among them, Calmodulin (CaM) is a key and ubiquitous  $\text{Ca}^{2+}$  sensor that modulates RyR2 directly through controlled activation of

RyR2 kinases. Mg<sup>2+</sup> can reduce the apparent Ca<sup>2+</sup> affinity of CaM, thus affecting its ability to bind to and regulate its multiple targets [20,109].

Among the numerous kinases activated by Ca<sup>2+</sup>-bound CaM, the delta isoform of the Ca<sup>2+</sup>/calmodulin-dependent protein kinase II (CaMK2d) is a critical modulator of cardiac RyR2. Physiologically, CaMK2d permits ventricular myocytes to adapt its AP and ECC machinery to increases in heart rate. However, when pathologically hyperactive, CaMK2d is involved in the pro-arrhythmogenic effects of catecholaminergic stimulation in the heart, in part mediated by phosphorylation of the target RyR2 residues Ser2814 (Ser2815 in large mammals) and Ser2808 (Ser2809 in the tested canine model), which enhances RyR2-mediated diastolic Ca<sup>2+</sup> release [110,111]. In resting myocytes, most CaMK2d is found near RyR2s. Upon pacing and binding of Ca<sup>2+</sup>/CaM to CaMK2d, a portion of the kinase diffuses away from Ca<sup>2+</sup> sources and longitudinally into the sarcomere, thus reaching a wider number of targets [112–114].

Here, the cycling variations in local Ca<sup>2+</sup> concentrations allow for transient binding of Mg<sup>2+</sup> at Ca<sup>2+</sup>-binding sites on CaMK2d, ultimately inhibiting the enzyme activity. Regarding instead a more general cytosolic mechanism, low Mg<sup>2+</sup> levels promote the phosphorylation of target Na<sup>+</sup> and Ca<sup>2+</sup> channels, including RyR2 [115,116].

In addition to CaMK2d, the cAMP-dependent protein kinase A (PKA) also necessitates Mg-ATP to efficiently phosphorylate RyR2 [117]. The crystallographic PKA–RyR2 peptide complex (PDB ID: 6MM5), where Mg<sup>2+</sup> coordinates the ATP at the PKA active site, is the only Mg<sup>2+</sup>-containing published structure where RyR2 appears. Similarly to Camk2d, PKA activity on multiple serines of RyR2 leads to uncoupling of the channel open probability from cytosolic Ca<sup>2+</sup> inactivation, which in turn facilitates SR calcium leak [118–120]. In mice, the only two sites where PKA-dependent RyR2 phosphorylation have been found to be of physiological relevance are S2808 (S2809 in large mammals) and S2030 [76,83,121,122].

Crucially, β-adrenergic stimulation, which increases RyR2 phosphorylation by CaMK2d and PKA at key sites such as S2808, S2814, and S2030, significantly diminishes the inhibitory effects of both luminal and cytoplasmic Mg<sup>2+</sup> on RyR2 activity [8,79,95]. This phosphorylation-dependent reduction in Mg<sup>2+</sup> inhibition is particularly evident in heart failure, where RyR2 hyperphosphorylation correlates with decreased channel sensitivity to cytoplasmic Mg<sup>2+</sup> [95]. In addition, it has been shown that a sizable Mg<sup>2+</sup> extrusion occurs in ventricular myocytes within minutes of β-adrenergic stimulation [123], which could further contribute to the β-adrenergic-stimulation-dependent increase in the apparent RyR2 affinity for Ca<sup>2+</sup> in intact cells.

### 5.3. Luminal Modulation of RyR2

It is unequivocally established that luminal Mg<sup>2+</sup> is a potent inhibitor of cardiac RyR2 activity. Mechanistically, two pathways have been proposed: Mg<sup>2+</sup> may flow through the channel to bind the cytosolic A-site, thereby preventing further channel activation by Ca<sup>2+</sup>, or bind directly to luminal sites to inhibit gating [86]. However, multiple studies indicate that the magnitude of the former “feed-through” mechanism is unlikely to be an efficient driver of the store-load dependence of RyR2 opening *in vivo* [27,86]. Experimental evidence, primarily obtained using RyR2 samples preserving associated luminal proteins such as calsequestrin (CASQ2), triadin (TRDN), and junctin (JNT), unveiled the role of the so-called L-site, an activation site for luminal Ca<sup>2+</sup>, at which luminal Mg<sup>2+</sup> competes as a non-activating antagonist [12,100]. Here, luminal Mg<sup>2+</sup> reduces the sensitivity of RyR2 to cytosolic Ca<sup>2+</sup> and caffeine-mediated activation, requiring higher concentrations of these cytosolic activators to achieve channel opening [27]. This competition shifts the Ca<sup>2+</sup> dose-response toward higher luminal Ca<sup>2+</sup> and serves as a critical physiological brake to prevent diastolic SR Ca<sup>2+</sup> leak [12,86]. Of particular note, unlike cytosolic Mg<sup>2+</sup> inhibition

(which is dominant in RyR1 but significantly weaker in RyR2), luminal  $Mg^{2+}$  exerts a more specific and potent inhibitory effect on RyR2. This highlights the importance, in the cardiac setting, of those  $Mg^{2+}$ -dependent mechanisms specifically occurring within the jSR lumen.

In the following paragraphs we will delve into how luminal  $Mg^{2+}$  regulates the open probability of RyR2 either in presence or absence of its soluble accessory protein CASQ2. Intriguingly, these two mechanisms, featuring distinct selectivities for  $Ca^{2+}$  vs.  $Mg^{2+}$  ions and different magnitudes of their physiological impacts, also feature opposite functional outcomes on RyR2.

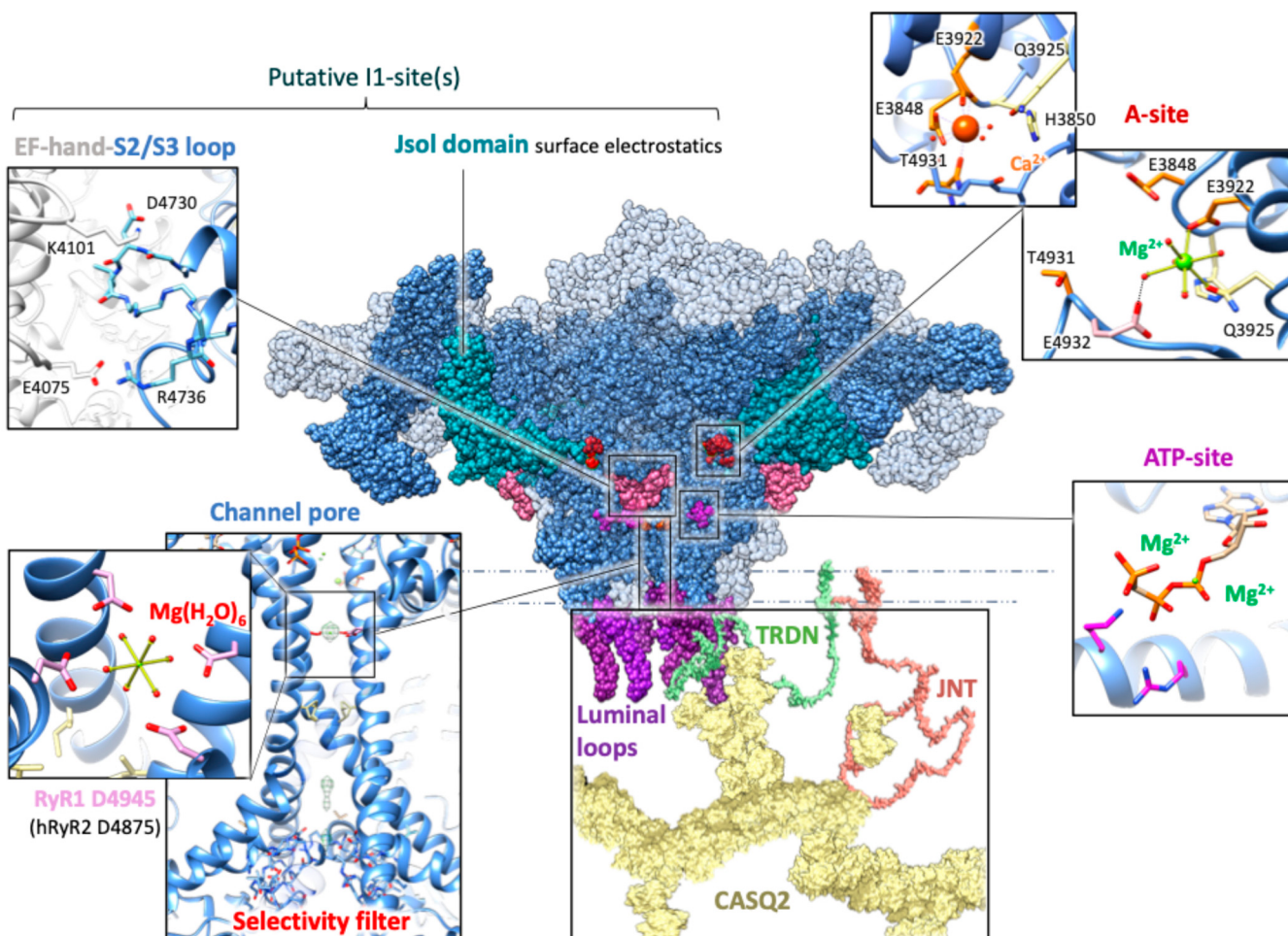


**Figure 2.** The structural landscape of  $Ca^{2+}$ / $Mg^{2+}$  binding sites in RyR2. The central panel shows the human cardiac ryanodine receptor type 2 (RyR2) structure (PDB ID: 7UA5 [124]) in its closed conformation, with two of the four monomers displayed as semi-transparent to enhance visualization of internal domains. The **A-site** (highlighted in red on the RyR2 structure): Distinct binding mechanisms are shown in the relative panels. In the open RyR2 structure (PDB ID: 7UA9 [124]), cytoplasmic  $Ca^{2+}$  is directly coordinated by the carboxylate side chains of Glu3848 (E3848) and Glu3922 (E3922) from the core domain and the backbone carbonyl of Thr4931 (T4931) from the C-terminal domain, with Gln3925 (Q3925) and His3850 (H3850) contributing to the second coordination sphere.  $Ca^{2+}$  binding promotes separation between the central and C-terminal domains, stabilizing the highly active open state. In contrast,  $Mg^{2+}$  binding has been experimentally visualized only in RyR1 (PDB ID: 7UMZ [84]). Given the conservation of residues, residue numbering here refers to human RyR2. In RyR1,  $Mg^{2+}$  coordinates predominantly with Glu3967 and Gln3970 (corresponding to RyR2 Glu3922 and Gln3925), and indirectly with Glu5002 (RyR2 Glu4932) via a water molecule, remaining separated

from Glu3893 (RyR2 Glu3848). This distinct  $Mg^{2+}$  coordination results in minimal conformational changes, insufficient to trigger channel activation. The **I1-site** inhibitory mechanism expectedly involves either one or both of two domains: the EF-hand/S2-S3 loop interface (pink), stabilized by salt bridges in the  $Mg^{2+}$ -triggered closed RyR1 conformation (PDB ID: 7UMZ [84]), and the Jsol (handle) domain (teal blue), with a highly charged surface favorable for divalent cation binding. The **ATP-binding site** (magenta) is detailed in the corresponding panel, showing two  $Mg^{2+}$  ions coordinating ATP as resolved in RyR1 under high- $Mg^{2+}$  conditions (PDB ID: 7UMZ [84]). The **channel pore**: In RyR1 (PDB ID: 7UMZ [84]), a hydrated  $Mg^{2+}$  ion is identified, positioned to form an octahedral water shell coordinated by D4945 from each monomer (corresponding to D4875 in human RyR2), stabilizing the closed state. Nearby lies the **selectivity filter**, another conserved charged region where  $Ca^{2+}$  and  $Mg^{2+}$  may compete, as supported by small non-protein densities observed in the RyR1 cryo-EM map (EMD-26610 [84]). **Luminal loops** (purple) are shown, where intrinsic luminal  $Mg^{2+}$ -dependent activation occurs. The disordered first intraluminal loop (RyR2 residues 4524–4555), structurally unsolved, is graphically represented as an extended loop. Both intraluminal loops harbor potential interaction sites, with **CASQ2** (represented using PDB ID 6OWW [125]) and **TRDN** mediating voltage-independent, luminal- $Mg^{2+}$ -dependent inactivation. The functional outcome of RyR2 physiological interaction with JNT is less understood.

### 5.3.1. $Mg^{2+}$ Direct Binding at RyR2 Luminal Site(s) Cooperates with $Ca^{2+}$ Activation

When RyR2 is stripped of CASQ2, maximally activating concentrations of cytosolic  $Ca^{2+}$  (100  $\mu$ M) unmask an intrinsic luminal  $Mg^{2+}$ -activation mechanism, where luminal  $Mg^{2+}$  is equally efficient as luminal  $Ca^{2+}$  in sustaining RyR2 channel opening, with an EC50 for  $Ca^{2+}/Mg^{2+}$  activation of  $379 \pm 247 \mu$ M [27,103]. More recently, Magyar et al., by probing at diastolic cytosolic  $Ca^{2+}$  (100 nM) levels with a non-permeating ion ( $Eu^{3+}$ ), corroborated the existence of an intrinsic luminal  $Ca^{2+}$ -activating site in canine RyR2 [100].

It is interesting to observe here that, differently from RyR2, the genuine luminal  $Ca^{2+}$ -binding site of the skeletal channel has an inhibitory effect [100]. In addition, while the  $Ca^{2+}$  affinity of the RyR2 L-site does not depend on voltage, the effect of cation binding at the RyR1 luminal site is voltage-dependent. Because of this non-conserved mechanism, two distinct locations have been proposed for the intrinsic L-sites of both the cardiac and skeletal channel isoforms. The luminal  $Ca^{2+}/Mg^{2+}$ -dependent inhibition of RyR2 is proposed to be mediated by a region outside the membrane's electric field. The EF-hand pattern found specifically within RyR2's first intraluminal loop (connecting the transmembrane helices S1 and S2) features this requirement and the absence of divalent cation selectivity [100,101]. On the contrary, the voltage-sensitive RyR1 inhibitory luminal site appears to be situated within the channel pore. On these premises, the intrinsic L-site of the skeletal channel has been proposed to involve the selectivity filter: a negatively charged, conserved GGGIG motif (lying within the S5–S6 luminal loop) exposed at the luminal mouth of the channel pore [100].

Recent studies also unveiled an additional, intrinsic, RyR2 luminal  $Ca^{2+}$ -binding site or  $Ca^{2+}$ -dependent allosteric mechanism which becomes apparent only under particular cytosolic  $Ca^{2+}$  concentrations and is otherwise of questionable functional importance [100]. The location of this site has been proposed to be conserved between isoforms: close to the channel gate and the selectivity filter. However, there are currently neither functional nor structural data on the effect here played by  $Mg^{2+}$ : while cryo-EM analysis of RyR1 shows an axial non-protein density in the conserved selectivity filter region, its density did not increase with  $Mg^{2+}$  concentration [84].

### 5.3.2. RyR2 Inhibition by Luminal $Mg^{2+}$ Is Mediated by IDR-Containing Proteins

Since the effects of luminal  $Mg^{2+}$  on RyR2 in the absence of protein partners are not specific to  $Ca^{2+}$  or  $Mg^{2+}$ , and their physiological meaning is only evident in special circumstances, the presence of luminal protein partners is the missing link to mechanisti-

cally explain the well-known, physiologically relevant RyR2 inhibition by luminal Mg<sup>2+</sup> (Figure 2). Partners ensure that RyR2 is capable of discriminating between luminal Ca<sup>2+</sup> (which activates RyR2 when interacting with partners) and luminal Mg<sup>2+</sup> (crucial to prevent excessive Ca<sup>2+</sup> release, particularly during diastole when cytoplasmic Ca<sup>2+</sup> concentrations are low and the SR is well loaded with Ca<sup>2+</sup>) [12,86,98]. Furthermore, in a context where the physiological concentration of luminal Mg<sup>2+</sup> is considered to stably remain at approximately 1 mM (due to the absence of well-established active Mg<sup>2+</sup> transport across the SR membrane), the discrimination between divalent cations is also necessary to ensure that the RyR2 activity is coupled with physiological fluctuations in the luminal free Ca<sup>2+</sup> content between 0.3 and 1 mM [3,86]. In addition, while partner-independent mechanisms alter the maximal efficacy of cytosolic Ca<sup>2+</sup>-dependent activation of RyR2, the CASQ2-dependent mechanism modulates the sensitivity to cytosolic Ca<sup>2+</sup> [103].

Crucially, only in presence of all its physiological protein partners (TRDN, JNT, and CASQ2), RyR2 is sensitive to both luminal Ca<sup>2+</sup> and Mg<sup>2+</sup>, with comparable affinities of 35–45 μM [126]. Mechanistically, competing luminal Mg<sup>2+</sup> shifts the K<sub>a</sub> for luminal Ca<sup>2+</sup> activation to 1 mM, close to the physiological variations in luminal Ca<sup>2+</sup>.

Notably, all members of the RyR2 macromolecular complex interact through their intrinsically disordered regions (IDRs) within the jSR lumen, with the globular core of CASQ2 representing a structured exception. Of note is the fact that the extended and structurally unresolved first luminal loop of RyR2 (connecting transmembrane helices S1–S2) may also contribute to this unstructured signaling hotspot [100,127]. The fascinating biochemical nature of the intricate interactions between RyR2 and its physiological partners is dissected below.

### 5.3.3. CASQ2

While free luminal Ca<sup>2+</sup> cycles in the 0.3–1 mM range, Ca<sup>2+</sup> ions in the jSR actually total 19 mM [1]. This impressive storage capacity builds upon the multiple low-affinity Ca<sup>2+</sup>-binding sites of a highly acidic protein, namely CASQ2. The significant proportion of aspartate and glutamate residues, of which half are concentrated in its C-terminal tail, endows CASQ2 with the ability to bind up to 60 ions per 45 kDa monomer while assembling into its functionally relevant, polymeric form [128,129]. CASQ2 is tethered to its jSR transmembrane partners TRDN and JNT [130,131], and inhibits RyR2 channel activity, with maximal inhibition at 1 mM Ca<sup>2+</sup>. In line with the physiological trend of Mg<sup>2+</sup> competition for Ca<sup>2+</sup>-binding sites, Mg<sup>2+</sup> reduces the number of Ca<sup>2+</sup> ions bound to CASQ2 [131,132], implying that Mg<sup>2+</sup> could indirectly impact the functionality of CASQ2 within the RyR2 complex and ultimately affect jSR Ca<sup>2+</sup> buffering and release dynamics [133]. Notably, Mg<sup>2+</sup> has been shown to “prime”, by an unknown molecular mechanism, recombinant CASQ2 for efficient Ca<sup>2+</sup>-dependent polymerization. Collectively analyzed, published insights demonstrating the dominant role of CASQ2’s disordered C-terminal portion on the protein polymerization responsiveness to Ca<sup>2+</sup> [134], and on its interaction with RyR2 [135], can be interpreted as indicating that the main functional outcomes of Ca<sup>2+</sup>/Mg<sup>2+</sup> competition are determined at this domain of the protein. This said, new studies are needed to further strengthen this interpretation.

Importantly, and unlike the RyR2-intrinsic L-site, the CASQ2-mediated regulation mechanism of RyR2 distinguishes between luminal Ca<sup>2+</sup> and Mg<sup>2+</sup>, as variations in luminal Ca<sup>2+</sup>, but not in luminal Mg<sup>2+</sup>, alter the cytosolic Ca<sup>2+</sup> sensitivity of the channel [103]. There is no clear consensus regarding the specific site of binding between CASQ2 and RyR2, the possible involvement of direct Mg<sup>2+</sup> binding, or its proximity to the intrinsic L-site (whose activating effect is masked by CASQ2-dependent inhibition) [104,120,130,136,137].

The prevailing understanding is that CASQ2 modulates RyR2 activity in a  $\text{Ca}^{2+}$ -dependent manner through its physical interactions with TRDN [35,103,138].

#### 5.3.4. TRDN and JNT

TRDN and JNT are single-pass transmembrane proteins which homologous, extended, and highly flexible luminal tails both possess multiple KEKE (Lys-Glu-Lys-Glu) motifs, believed to be the primary binding sites for  $\text{Ca}^{2+}$ , RyR2, and CASQ2 [139,140]. They are not only essential for anchoring CASQ2 to the jSR membrane, but also for luminal  $\text{Ca}^{2+}$  sensing and propagation of conformational changes across the RyR2 protein complex [136,141–143]. On the RyR2 side, the site for interaction with TRD and JNT is presumed to lie within the second intraluminal loop, particularly conserved and rich in charged amino acids [35]. However, in RyR1 it has been demonstrated that the C-terminal loop is also essential [105]. Notably, while the interaction between TRDN and JNT with RyR2 is  $\text{Ca}^{2+}$ -independent [35], their interaction with CASQ2 is inhibited by increasing  $\text{Ca}^{2+}$  amounts [137]. Of note, while the role of cardiac TRDN in physically tethering CASQ2 to the RyR2 complex is solidly demonstrated [134], the role of JNT is far less evident. One study even reported that JNT does not directly interact with CASQ2 [144]. What is known regarding the role of JNT in the cardiac setting is that it indirectly supports proper CASQ2 anchoring at the jSR membrane, and that its overexpression leads to narrowing and extension of the jSR portion [145]. Because of its poor relevance in the cardiac myocytes (counteracted by a more conspicuous effect in the skeletal scenario), we will not dissect its properties further.

#### 5.3.5. The Functional Relevance of Luminal IDRs in the RyR2 Complex

Either TRDN or CASQ2 knockout leads to severe architectural disorganization of jSR cisternae, and a notable reduction in the levels of the counterpart protein: CASQ2 in the case of TRDN KO, and TRDN in the case of CASQ2 KO. Both these situations lead to impaired  $\text{Ca}^{2+}$  homeostasis and enhanced RyR2 sensitivity to cytosolic  $\text{Ca}^{2+}$  activation [108,136,146–148], which in turn couples with the development of CPVT, a highly severe hereditary arrhythmogenic disorder [103,149–151].

All this evidence for the profound functional link between TRDN and CASQ2 points to the fact that there exists at least a partial superposition among their mechanisms of interaction with RyR2. In the case of TRDN, the molecular basis of this functional link can only be attributed to its long and disordered luminal segment. Interestingly, concerning the mechanism employed by CASQ2 for  $\text{Ca}^{2+}$ -dependent RyR2 modulation, what is known is that the electrostatics of its C-terminal IDR integrates the sensitivity to multiple ions ( $\text{Ca}^{2+}$  and  $\text{Mg}^{2+}$ ) within the dynamics of the functional interactions between CASQ2 monomers [125,133] and expectedly between CASQ2 and the TRDN-RyR2 complex [134,140]. Further supporting the relevance of the C-terminal IDR and of its multiple dynamic interactions with the globular core, CPVT-causative missense CASQ2 mutations are spread all over the negative surface of CASQ2, with the specific exception of this C-terminal segment [130]. Overall, it appears that the highly electrostatic IDRs exposed by CASQ2 and TRDN funnel the multiple  $\text{Ca}^{2+}$ / $\text{Mg}^{2+}$ -competitive binding events into a defined set of (expectedly similar) mechanisms for direct and/or indirect RyR2 modulation.

## 6. Pathological Dysregulation of $\text{Mg}^{2+}$ and Therapeutic Implications

The tightly controlled and delicate balance of intracellular free  $\text{Mg}^{2+}$  is critical, and deviations in either direction (hypomagnesemia or hypermagnesemia) have profound pathological implications.  $\text{Mg}^{2+}$  is one of the few ions used as a first-line treatment in emergency cardiovascular care: intravenous magnesium sulfate is administered for Torsades de

pointes and other ventricular arrhythmias, and shows potential in long-term heart failure and hypertension management and as a metabolic stabilizer in diabetes [10].

### 6.1. Hypomagnesemia and Associated Disorders

Hypomagnesemia (commonly defined as serum  $Mg^{2+} < 0.8$  mM) is increasingly recognized as a widespread and underdiagnosed condition [152]. Given that serum  $Mg^{2+}$  represents only ~1% of total body magnesium, patients can be in a  $Mg^{2+}$ -depleted state even with normal serum levels and remain asymptomatic until serum  $Mg^{2+}$  falls below 0.5 mM, highlighting why the clinical impact of magnesium deficiency may be underestimated [152]. Signs of hypomagnesemia include generalized weakness to cardiac ischemia and death. Hypomagnesemia is also prevalent in metabolic (diabetes and obesity) and neuromuscular disorders [10,153,154]. In the skeletal muscle, pathological RyR regulation and oxidative stress are exacerbated by  $Mg^{2+}$  deficiency [155]. Also, since  $Mg^{2+}$  exerts a vasodilatory effect on vascular smooth muscle, its deficiency promotes vasoconstriction and hypertension [48]. The number of consequences of hypomagnesemia are due to the multiple pathways affected by  $Mg^{2+}$  within each tissue, which could secondarily affect heart function.

More specifically for the heart, hypomagnesemia alters not only the contractile force of the actin–myosin system, but also the handling of the electrical signal and ECC (Figure 3). The overall outcome on cardiac health mainly falls into two conditions:

- Heart Failure (HF): Chronic heart failure is often associated with reduced intracellular free  $Mg^{2+}$ . In a canine pacing-induced HF model,  $[Mg^{2+}]_i$  was reduced by ~50% in failing cardiomyocytes [156], leading to enhanced  $Ca^{2+}$  influx, slower inactivation, and increased susceptibility to  $Ca^{2+}$  overload, hypertrophy, and arrhythmias [52]. Beyond  $Ca^{2+}$  handling,  $Mg^{2+}$  deficiency alters action potential dynamics. Depending on cell type and repolarization mechanisms, low  $[Mg^{2+}]_i$  levels can prolong AP duration by inhibiting  $K^+$  or prolonging  $Ca^{2+}$  currents [7,10]. These effects facilitate early (EADs) and delayed (DADs) afterdepolarizations, especially under  $\beta$ -adrenergic stimulation. Disease progression in HF is also due to the negative consequences of low  $Mg^{2+}$  on mitochondria (oxidative stress, inflammation, and metabolic dysfunction), partly through upregulation of the TRPM7 kinase-channel [5].
- Arrhythmias:  $Mg^{2+}$  deficiency prolongs AP duration by affecting  $K^+$  and  $Ca^{2+}$  currents and, as shown in Section 5, increases RyR2 diastolic leak (Figure 3) [1]. These changes increase susceptibility to EADs and DADs, Torsades de pointes [60], atrial fibrillation and CPVT [48]. In CPVT, defective regulation of RyR2—often due to mutations in calsequestrin (CASQ2)—is compounded by low  $Mg^{2+}$  levels, worsening the arrhythmic phenotype [157].

### 6.2. Ischemia-Associated Hypermagnesemia

Although clinically less common, during transient ischemia, intracellular  $Mg^{2+}$  rises two- to three-fold due to ATP hydrolysis [158], leading to potent inhibition of L-type  $Ca^{2+}$  currents and accelerated inactivation [52]. This  $Mg^{2+}$ -mediated inhibition of Cav1.2, coupled with depressed myofilament  $Ca^{2+}$  sensitivity and ATPase activity, serves as a cell-autonomous protective mechanism, reducing  $Ca^{2+}$  influx, contractile demand, and metabolic burden in affected myocytes while sparing neighboring healthy cells [159].

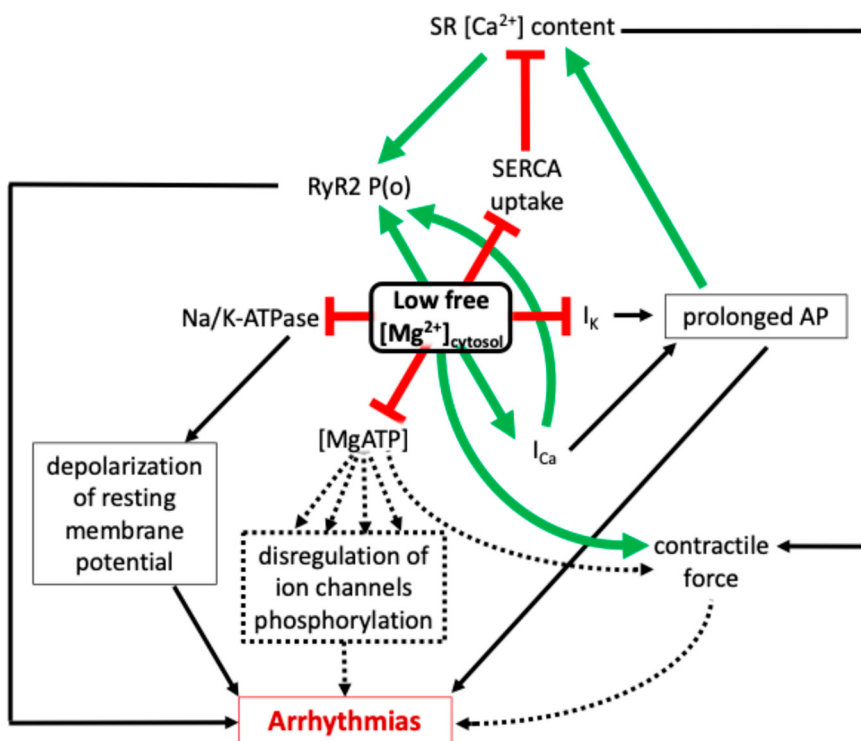


**Figure 3.** Integrated effects of low cytosolic free magnesium concentration ( $[Mg^{2+}]_{cytosol}$ ) on cardiac ECC and arrhythmogenesis. The green arrows indicate positive (enhancing) effects; red bars indicate inhibitory effects; and dotted arrows represent indirect regulatory pathways for which only the net positive/negative effect has not been precisely determined. This multifaceted disturbance underscores the essential role of  $Mg^{2+}$  homeostasis in maintaining cardiac electrical and contractile stability. Low intracellular free  $Mg^{2+}$  profoundly alters cardiac physiology at multiple levels. At the membrane level, it enhances L-type  $Ca^{2+}$  current ( $I_{Ca}$ ) and suppresses repolarizing  $K^{+}$  currents ( $I_K$ ), contributing to prolonged action potential duration (APD). APD prolongation facilitates increased  $Ca^{2+}$  influx and sarcoplasmic reticulum (SR)  $Ca^{2+}$  content. In parallel, low  $Mg^{2+}$  enhances RyR2 open probability ( $P_o$ ) by relieving  $Mg^{2+}$ -dependent inhibition at both cytosolic and luminal  $Ca^{2+}$  regulatory sites, further promoting SR  $Ca^{2+}$  leak. Low  $[Mg^{2+}]_{cytosol}$  also reduces the pool of usable MgATP, which is essential for the activity of several ATPases. Decreased MgATP impairs SERCA-mediated  $Ca^{2+}$  reuptake into the SR and diminishes  $Na^{+}/K^{+}$ -ATPase activity, leading to membrane depolarization and destabilization of ionic gradients. MgATP scarcity also disrupts kinase/phosphatase activity and ion channel phosphorylation states, compounding electrical instability. In the myofilament compartment, reduced  $Mg^{2+}$  increases the  $Ca^{2+}$  sensitivity of troponin C by decreasing competitive inhibition, potentially enhancing contractile force. However, impaired  $Ca^{2+}$  reuptake due to SERCA inhibition and RyR2 leak can deplete SR  $Ca^{2+}$  reserves over time, compromising systolic  $Ca^{2+}$  transients and contractile efficiency. The net result is a paradoxical state where increased  $Ca^{2+}$  release coexists with impaired relaxation and energy imbalance, predisposing to arrhythmias.

## 7. Conclusions

Endowed with a high charge density and a massive solvation sphere,  $Mg^{2+}$  ions have difficulties in stably binding to flexible protein binding sites. Coordination with  $Mg^{2+}$  is rigid and energetically costly, making  $Mg^{2+}$  unsuitable for signaling functions such as cardiac ECC. This signaling role is ultimately performed by  $Ca^{2+}$ , a more flexible bivalent with lesser desolvation requirements and a promiscuous coordination, which allows proteins to flexibly change conformation upon ion (un-)binding. That said,  $Mg^{2+}$  exerts surprisingly strong effects on cardiac ECC, either in the form of direct regulation (e.g., IK1 rectification, RyR2 inhibition by competition with  $Ca^{2+}$ ) or much subtler pathways, such as alteration of protein distribution (e.g., changes in JPH2 conformation and RyR2 disposition), control of protein expression (e.g., Kir4.2 and 2.1), and indirectly via Mg-ATP

availability, which impacts resting membrane potential, RyR2 proneness to open (via ATP site), and overall channel phosphorylation. Three thrilling frontiers to be researched further are the elucidation of the Mg<sup>2+</sup>-dependent interaction with SR luminal disordered regions (such as those within CASQ2 and TRDN); structural determinants of Mg<sup>2+</sup> interactions with RyR2; and how such Mg<sup>2+</sup>-dependent interactions play a pro-arrhythmogenic role in diseased states. While the leading role of Ca<sup>2+</sup> in cardiac ECC cannot be overstated, the quiet and steady antagonistic action of Mg<sup>2+</sup> provides what cardiac cells need most: robustness and stability.

**Author Contributions:** Conceptualization, C.M. and D.J.S.; writing—review and editing, C.M., D.J.S., and S.G.P. All authors have read and agreed to the published version of the manuscript.

**Funding:** This work was supported by Fondazione Telethon ETS—Italy (Grant no. GMR24T1117).

**Data Availability Statement:** No new data were created or analyzed in this study. Data sharing is not applicable to this article.

**Acknowledgments:** We acknowledge the support of Fondazione della Comunità della Provincia di Pavia for the NanoTrac Flex instrument (© 2025 Microtrac Retsch GmbH).

**Conflicts of Interest:** The authors declare no conflicts of interest.

## Abbreviations

The following abbreviations are used in this manuscript:

AP	Action Potential
ATP	Adenosine Triphosphate
CaM	Calmodulin
CaMK2d	Ca <sup>2+</sup> /Calmodulin-Dependent Protein Kinase II Delta Isoform
CASQ2	Calsequestrin 2
Cav1.2	L-Type Calcium Channel Isoform
CICR	Calcium-Induced Calcium Release
CPVT	Catecholaminergic Polymorphic Ventricular Tachycardia
cTnC	Cardiac Troponin C
ECC	Excitation–Contraction Coupling
EC50	Half Maximal Effective Concentration
EF-hand	Helix–Loop–Helix Structural Domain (Calcium-Binding Motif)
HF	Heart Failure
IC50	Half Maximal Inhibitory Concentration
ICaL	L-Type Calcium Current
IK1	Inward Rectifier Potassium Current
IKr	Rapid Delayed Rectifier Potassium Current
IKs	Slow Delayed Rectifier Potassium Current
INa	Rapid Depolarizing Sodium Current
Ito	Transient Outward Potassium Current
JNT	Junctin
JPH2	Junctophilin 2
jSR	Junctional Sarcoplasmic Reticulum
Kir2.1	Potassium Channel Isoform Underlying IK1
Kv4.2	Potassium Channel Isoform Underlying Ito
Mg-ATP	Magnesium–ATP Complex
Nav1.5	Cardiac Sodium Channel Isoform
NCX	Sodium–Calcium Exchanger
PKA	Protein Kinase A
PLB	Phospholamban
P <sub>o</sub>	Open Probability

PtdIns(3,4,5)P3	Phosphatidylinositol (3,4,5)-Trisphosphate
RyR1	Ryanodine Receptor Type 1
RyR2	Ryanodine Receptor Type 2
SERCA	Sarco/Endoplasmic Reticulum $\text{Ca}^{2+}$ -ATPase
SR	Sarcoplasmic Reticulum
SUMOylase	Small Ubiquitin-Like Modifier enzyme
TRDN	Triadin

## References

- Bers, D.M. *Excitation-Contraction Coupling and Cardiac Contractile Force*, 2nd ed.; Developments in cardiovascular medicine; Kluwer Academic Publishers: Dordrecht, The Netherlands; Boston, MA, USA, 2001; ISBN 978-0-7923-7157-1.
- Laver, D.R. Coupled Calcium Release Channels and Their Regulation by Luminal and Cytosolic Ions. *Eur. Biophys. J.* **2005**, *34*, 359–368. [CrossRef] [PubMed]
- Bers, D.M. Cardiac Excitation-Contraction Coupling. *Nature* **2002**, *415*, 198–205. [CrossRef] [PubMed]
- White, R.E.; Hartzell, H.C. Magnesium Ions in Cardiac Function. *Biochem. Pharmacol.* **1989**, *38*, 859–867. [CrossRef]
- Liu, M.; Dudley, S.C. Beyond Ion Homeostasis: Hypomagnesemia, Transient Receptor Potential Melastatin Channel 7, Mitochondrial Function, and Inflammation. *Nutrients* **2023**, *15*, 3920. [CrossRef]
- Michailova, A.P.; Belik, M.E.; McCulloch, A.D. Effects of Magnesium on Cardiac Excitation-Contraction Coupling. *J. Am. Coll. Nutr.* **2004**, *23*, 514S–517S. [CrossRef]
- Agus, Z.S.; Morad, M. Modulation of cardiac ion channels by magnesium. *Annu. Rev. Physiol.* **1991**, *53*, 299–307. [CrossRef]
- Wang, M.; Berlin, J.R. Channel Phosphorylation and Modulation of L-Type  $\text{Ca}^{2+}$  Currents by Cytosolic  $\text{Mg}^{2+}$  Concentration. *Am. J. Physiol. Cell Physiol.* **2006**, *291*, C83–C92. [CrossRef]
- Rios, F.J.; Montezano, A.C.; Antunes, T.T.; Touyz, R.M. Chapter 29—Magnesium, Vascular Function, and Hypertension. In *Molecular, Genetic, and Nutritional Aspects of Major and Trace Minerals*; Collins, J.F., Ed.; Academic Press: Boston, MA, USA, 2017; pp. 353–364, ISBN 978-0-12-802168-2.
- Fritzen, R.; Davies, A.; Veenhuizen, M.; Campbell, M.; Pitt, S.J.; Ajjan, R.A.; Stewart, A.J. Magnesium Deficiency and Cardiometabolic Disease. *Nutrients* **2023**, *15*, 2355. [CrossRef]
- Murphy, R.M.; Larkins, N.T.; Mollica, J.P.; Beard, N.A.; Lamb, G.D. Calsequestrin Content and SERCA Determine Normal and Maximal  $\text{Ca}^{2+}$  Storage Levels in Sarcoplasmic Reticulum of Fast- and Slow-Twitch Fibres of Rat. *J. Physiol.* **2009**, *587*, 443–460. [CrossRef]
- Walweel, K.; Li, J.; Molenaar, P.; Imtiaz, M.S.; Quail, A.; Dos Remedios, C.G.; Beard, N.A.; Dulhunty, A.F.; Van Helden, D.F.; Laver, D.R. Differences in the Regulation of RyR2 from Human, Sheep, and Rat by  $\text{Ca}^{2+}$  and  $\text{Mg}^{2+}$  in the Cytoplasm and in the Lumen of the Sarcoplasmic Reticulum. *J. Gen. Physiol.* **2014**, *144*, 263–271. [CrossRef]
- Wang, M.; Tashiro, M.; Berlin, J.R. Regulation of L-type Calcium Current by Intracellular Magnesium in Rat Cardiac Myocytes. *J. Physiol.* **2004**, *555*, 383–396. [CrossRef]
- Zocchi, M.; Bartolini, M.; Maier, J.A.; Castiglioni, S. Low Extracellular Magnesium Induces Phenotypic and Metabolic Alterations in C2C12-Derived Myotubes. *Sci. Rep.* **2023**, *13*, 19425. [CrossRef]
- Pilchova, I.; Klacanova, K.; Tatarkova, Z.; Kaplan, P.; Racay, P. The Involvement of  $\text{Mg}^{2+}$  in Regulation of Cellular and Mitochondrial Functions. *Oxid. Med. Cell. Longev.* **2017**, *2017*, 6797460. [CrossRef] [PubMed]
- Grauffel, C.; Dudev, T.; Lim, C. Why Cellular Di/Triphosphates Preferably Bind  $\text{Mg}^{2+}$  and Not  $\text{Ca}^{2+}$ . *J. Chem. Theory Comput.* **2019**, *15*, 6992–7003. [CrossRef] [PubMed]
- Lai, L.T.F.; Balaraman, J.; Zhou, F.; Matthies, D. Cryo-EM Structures of Human Magnesium Channel MRS2 Reveal Gating and Regulatory Mechanisms. *Nat. Commun.* **2023**, *14*, 7207. [CrossRef] [PubMed]
- Azzam, A.M. Theoretical studies on solvation: Part II. New theory for evaluation of ionic solvation number for divalent ions at 25 °C. *Can. J. Chem.* **1960**, *38*, 993–1002. [CrossRef]
- Maguire, M.E.; Cowan, J.A. Magnesium Chemistry and Biochemistry. *Biometals* **2002**, *15*, 203–210. [CrossRef]
- Ohki, S.; Ikura, M.; Zhang, M. Identification of  $\text{Mg}^{2+}$ -Binding Sites and the Role of  $\text{Mg}^{2+}$  on Target Recognition by Calmodulin. *Biochemistry* **1997**, *36*, 4309–4316. [CrossRef]
- Rayani, K.; Hantz, E.R.; Haji-Ghassemi, O.; Li, A.Y.; Spuches, A.M.; Van Petegem, F.; Solaro, R.J.; Lindert, S.; Tibbits, G.F. The Effect of  $\text{Mg}^{2+}$  on  $\text{Ca}^{2+}$  Binding to Cardiac Troponin C in Hypertrophic Cardiomyopathy Associated TNNC1 Variants. *FEBS J.* **2022**, *289*, 7446–7465. [CrossRef]
- Berman, H.M.; Westbrook, J.; Feng, Z.; Gilliland, G.; Bhat, T.N.; Weissig, H.; Shindyalov, I.N.; Bourne, P.E. The Protein Data Bank. *Nucleic Acids Res.* **2000**, *28*, 235–242. [CrossRef]
- Gifford, J.L.; Walsh, M.P.; Vogel, H.J. Structures and Metal-Ion-Binding Properties of the  $\text{Ca}^{2+}$ -Binding Helix-Loop-Helix EF-Hand Motifs. *Biochem. J.* **2007**, *405*, 199–221. [CrossRef]

24. Eisner, D.A.; Caldwell, J.L.; Kistamás, K.; Trafford, A.W. Calcium and Excitation-Contraction Coupling in the Heart. *Circ. Res.* **2017**, *121*, 181–195. [[CrossRef](#)] [[PubMed](#)]
25. Rog-Zielinska, E.A.; Moss, R.; Kaltenbacher, W.; Greiner, J.; Verkade, P.; Seemann, G.; Kohl, P.; Cannell, M.B. Nano-Scale Morphology of Cardiomyocyte t-Tubule/Sarcoplasmic Reticulum Junctions Revealed by Ultra-Rapid High-Pressure Freezing and Electron Tomography. *J. Mol. Cell. Cardiol.* **2021**, *153*, 86–92. [[CrossRef](#)] [[PubMed](#)]
26. Lamb, G. Excitation–Contraction Coupling In Skeletal Muscle: Comparisons with Cardiac Muscle. *Clin. Exp. Pharmacol. Physiol.* **2000**, *27*, 216–224. [[CrossRef](#)] [[PubMed](#)]
27. Diaz-Sylvester, P.L.; Porta, M.; Copello, J.A. Modulation of Cardiac Ryanodine Receptor Channels by Alkaline Earth Cations. *PLoS ONE* **2011**, *6*, e26693. [[CrossRef](#)]
28. Bers, D.M. Macromolecular Complexes Regulating Cardiac Ryanodine Receptor Function. *J. Mol. Cell. Cardiol.* **2004**, *37*, 417–429. [[CrossRef](#)]
29. Choi, R.H.; Koenig, X.; Launikonis, B.S. Dantrolene Requires Mg<sup>2+</sup> to Arrest Malignant Hyperthermia. *Proc. Natl. Acad. Sci. USA* **2017**, *114*, 4811–4815. [[CrossRef](#)]
30. Zahradníková, A.; Dura, M.; Györke, I.; Escobar, A.L.; Zahradník, I.; Györke, S. Regulation of Dynamic Behavior of Cardiac Ryanodine Receptor by Mg<sup>2+</sup> under Simulated Physiological Conditions. *Am. J. Physiol. Cell Physiol.* **2003**, *285*, C1059–C1070. [[CrossRef](#)]
31. Santiago, D.J.; Curran, J.W.; Bers, D.M.; Lederer, W.J.; Stern, M.D.; Ríos, E.; Shannon, T.R. Ca Sparks Do Not Explain All Ryanodine Receptor-Mediated SR Ca Leak in Mouse Ventricular Myocytes. *Biophys. J.* **2010**, *98*, 2111–2120. [[CrossRef](#)]
32. Macquaide, N.; Tuan, H.-T.M.; Hotta, J.; Sempels, W.; Lenaerts, I.; Holemans, P.; Hofkens, J.; Jafri, M.S.; Willems, R.; Sipido, K.R. Ryanodine Receptor Cluster Fragmentation and Redistribution in Persistent Atrial Fibrillation Enhance Calcium Release. *Cardiovasc. Res.* **2015**, *108*, 387–398. [[CrossRef](#)]
33. Guo, T.; Wang, H.; Wu, F.; Lu, W.; Zhu, M.; Ma, S.; Zhang, Y.; Yan, Y.; Zhou, M.; Talanaite, D.; et al. Functional Analysis of JPH2-Knockout Cardiomyocytes Identifies ECCD as a Novel Indicator in a Human Cardiac modelJPH2. *Stem Cell Res. Ther.* **2025**, *16*, 234. [[CrossRef](#)]
34. Soeller, C.; Cannell, M.B. Numerical Simulation of Local Calcium Movements during L-Type Calcium Channel Gating in the Cardiac Diad. *Biophys. J.* **1997**, *73*, 97–111. [[CrossRef](#)] [[PubMed](#)]
35. Gyorke, S.; Terentyev, D. Modulation of Ryanodine Receptor by Luminal Calcium and Accessory Proteins in Health and Cardiac Disease. *Cardiovasc. Res.* **2007**, *77*, 245–255. [[CrossRef](#)] [[PubMed](#)]
36. Biesmans, L.; Macquaide, N.; Heinzel, F.R.; Bito, V.; Smith, G.L.; Sipido, K.R. Subcellular Heterogeneity of Ryanodine Receptor Properties in Ventricular Myocytes with Low T-Tubule Density. *PLoS ONE* **2011**, *6*, e25100. [[CrossRef](#)]
37. Venetucci, L.A.; Trafford, A.W.; Eisner, D.A. Increasing Ryanodine Receptor Open Probability Alone Does Not Produce Arrhythmogenic Calcium Waves: Threshold Sarcoplasmic Reticulum Calcium Content Is Required. *Circ. Res.* **2007**, *100*, 105–111. [[CrossRef](#)]
38. Baylor, S.M.; Hollingworth, S. Model of Sarcomeric Ca<sup>2+</sup> Movements, Including ATP Ca<sup>2+</sup> Binding and Diffusion, during Activation of Frog Skeletal Muscle. *J. Gen. Physiol.* **1998**, *112*, 297–316. [[CrossRef](#)]
39. Woldeyes, R.A.; Nishiga, M.; Roest, A.S.V.; Engel, L.; Giri, P.; Montenegro, G.C.; Dunn, A.R.; Spudich, J.A.; Bernstein, D.; Schmid, M.F.; et al. Structure of the Thin Filament in Human iPSC-Derived Cardiomyocytes and Its Response to Heart Disease. *bioRxiv* **2025**. [[CrossRef](#)]
40. Wang, X.; An, P.; Gu, Z.; Luo, Y.; Luo, J. Mitochondrial Metal Ion Transport in Cell Metabolism and Disease. *Int. J. Mol. Sci.* **2021**, *22*, 7525. [[CrossRef](#)]
41. Franzini-Armstrong, C. ER-Mitochondria Communication. How Privileged? *Physiology* **2007**, *22*, 261–268. [[CrossRef](#)]
42. Drum, B.M.; Yuan, C.; De La Mata, A.; Grainger, N.; Santana, L.F. Junctional Sarcoplasmic Reticulum Motility in Adult Mouse Ventricular Myocytes. *Am. J. Physiol. Cell Physiol.* **2020**, *318*, C598–C604. [[CrossRef](#)]
43. Maack, C.; O'Rourke, B. Excitation-Contraction Coupling and Mitochondrial Energetics. *Basic Res. Cardiol.* **2007**, *102*, 369–392. [[CrossRef](#)] [[PubMed](#)]
44. Csernoch, L.; Bernengo, J.C.; Szentesi, P.; Jacquemond, V. Measurements of Intracellular Mg<sup>2+</sup> Concentration in Mouse Skeletal Muscle Fibers with the Fluorescent Indicator Mag-Indo-1. *Biophys. J.* **1998**, *75*, 957–967. [[CrossRef](#)] [[PubMed](#)]
45. Steele, D.S.; Duke, A.M. Defective Mg<sup>2+</sup> Regulation of RyR1 as a Causal Factor in Malignant Hyperthermia. *Arch. Biochem. Biophys.* **2007**, *458*, 57–64. [[CrossRef](#)]
46. Romani, A.M.P. Effect of Acute and Prolonged Alcohol Administration on Mg<sup>2+</sup> Homeostasis in Cardiac Cells. *Alcohol* **2015**, *49*, 265–273. [[CrossRef](#)]
47. Liguori, S.; Moretti, A.; Paoletta, M.; Gimigliano, F.; Iolascon, G. Role of Magnesium in Skeletal Muscle Health and Neuromuscular Diseases: A Scoping Review. *Int. J. Mol. Sci.* **2024**, *25*, 11220. [[CrossRef](#)]
48. Mubagwa, K.; Gwanyanya, A.; Zakharov, S.; Macianskiene, R. Regulation of Cation Channels in Cardiac and Smooth Muscle Cells by Intracellular Magnesium. *Arch. Biochem. Biophys.* **2007**, *458*, 73–89. [[CrossRef](#)]

49. Zhang, S.; Sawanobori, T.; Adaniya, H.; Hirano, Y.; Hiraoka, M. Dual Effects of External Magnesium on Action Potential Duration in Guinea Pig Ventricular Myocytes. *Am. J. Physiol.* **1995**, *268*, H2321–H2328. [[CrossRef](#)]
50. Albitz, R.; Magyar, J.; Nilius, B. Block of Single Cardiac Sodium Channels by Intracellular Magnesium. *Eur. Biophys. J.* **1990**, *19*, 19–23. [[CrossRef](#)]
51. Brunet, S.; Scheuer, T.; Catterall, W.A. Modulation of CaV1.2 Channels by Mg<sup>2+</sup> Acting at an EF-Hand Motif in the COOH-Terminal Domain. *J. Gen. Physiol.* **2005**, *126*, 311–323. [[CrossRef](#)]
52. Brunet, S.; Scheuer, T.; Catterall, W.A. Cooperative Regulation of Cav1.2 Channels by Intracellular Mg<sup>2+</sup>, the Proximal C-Terminal EF-Hand, and the Distal C-Terminal Domain. *J. Gen. Physiol.* **2009**, *134*, 81–94. [[CrossRef](#)]
53. Brunet, S.; Scheuer, T.; Catterall, W.A. Increased Intracellular Magnesium Attenuates β-Adrenergic Stimulation of the Cardiac CaV1.2 Channel. *J. Gen. Physiol.* **2013**, *141*, 85–94. [[CrossRef](#)] [[PubMed](#)]
54. Gillespie, D.; Chen, H.; Fill, M. Is Ryanodine Receptor a Calcium or Magnesium Channel? Roles of K<sup>+</sup> and Mg<sup>2+</sup> during Ca<sup>2+</sup> Release. *Cell Calcium* **2012**, *51*, 427–433. [[CrossRef](#)]
55. Treinys, R.; Kanaporis, G.; Fischmeister, R.; Jurevičius, J. Metabolic Inhibition Induces Transient Increase of L-Type Ca<sup>2+</sup> Current in Human and Rat Cardiac Myocytes. *Int. J. Mol. Sci.* **2019**, *20*, 1501. [[CrossRef](#)]
56. Shimaoka, T.; Wang, Y.; Morishima, M.; Miyamoto, S.; Ono, K. Magnesium Deficiency Causes Transcriptional Downregulation of Kir2.1 and Kv4.2 Channels in Cardiomyocytes Resulting in QT Interval Prolongation. *Circ. J.* **2020**, *84*, 1244–1253. [[CrossRef](#)]
57. Sudo, G.Z.; Sanguinetti, M.C. Intracellular [Mg<sup>++</sup>] Determines Specificity of K<sup>+</sup> Channel Block by a Class III Antiarrhythmic Drug. *J. Pharmacol. Exp. Ther.* **1996**, *276*, 951–957. [[CrossRef](#)]
58. Hirahara, K.; Matsubayashi, T.; Matsuura, H.; Ehara, T. Intracellular Mg<sup>2+</sup> Depletion Depresses the Delayed Rectifier K<sup>+</sup> Current in Guinea Pig Ventricular Myocytes. *Jpn. J. Physiol.* **1998**, *48*, 81–89. [[CrossRef](#)]
59. Huang, C.-W.; Kuo, C.-C. A Synergistic Blocking Effect of Mg<sup>2+</sup> and Spermine on the Inward Rectifier K<sup>+</sup> (Kir2.1) Channel Pore. *Sci. Rep.* **2016**, *6*, 21493. [[CrossRef](#)]
60. Ishihara, K.; Sarai, N.; Asakura, K.; Noma, A.; Matsuoka, S. Role of Mg<sup>2+</sup> Block of the Inward Rectifier K<sup>+</sup> Current in Cardiac Repolarization Reserve: A Quantitative Simulation. *J. Mol. Cell. Cardiol.* **2009**, *47*, 76–84. [[CrossRef](#)]
61. Grandi, E.; Pasqualini, F.S.; Bers, D.M. A Novel Computational Model of the Human Ventricular Action Potential and Ca Transient. *J. Mol. Cell. Cardiol.* **2010**, *48*, 112–121. [[CrossRef](#)]
62. Dyckner, T.; Wester, P.O. Relation between Potassium, Magnesium and Cardiac Arrhythmias. *Acta Med. Scand. Suppl.* **1981**, *647*, 163–169. [[CrossRef](#)]
63. Wei, S.; Quigley, J.F.; Hanlon, S.U.; O'Rourke, B.; Haigney, M.C.P. Cytosolic Free Magnesium Modulates Na/Ca Exchange Currents in Pig Myocytes. *Cardiovasc. Res.* **2002**, *53*, 334–340. [[CrossRef](#)] [[PubMed](#)]
64. Smith, G.A.; Vandenberg, J.I.; Freestone, N.S.; Dixon, H.B.F. The Effect of Mg<sup>2+</sup> on Cardiac Muscle Function: Is CaATP the Substrate for Priming Myofibril Cross-Bridge Formation and Ca<sup>2+</sup> Reuptake by the Sarcoplasmic Reticulum? *Biochem. J.* **2001**, *354*, 539–551. [[CrossRef](#)] [[PubMed](#)]
65. Sun, B.; Stewart, B.D.; Kucharski, A.N.; Kekenes-Huskey, P.M. Thermodynamics of Cation Binding to the Sarcoendoplasmic Reticulum Calcium ATPase Pump and Impacts on Enzyme Function. *J. Chem. Theory Comput.* **2019**, *15*, 2692–2705. [[CrossRef](#)] [[PubMed](#)]
66. Mahaney, J.E.; Albers, R.W.; Waggoner, J.R.; Kutchai, H.C.; Froehlich, J.P. Intermolecular Conformational Coupling and Free Energy Exchange Enhance the Catalytic Efficiency of Cardiac Muscle SERCA2a Following the Relief of Phospholamban Inhibition. *Biochemistry* **2005**, *44*, 7713–7724. [[CrossRef](#)]
67. Kho, C.; Lee, A.; Jeong, D.; Oh, J.G.; Chaanine, A.H.; Kizana, E.; Park, W.J.; Hajjar, R.J. SUMO1-Dependent Modulation of SERCA2a in Heart Failure. *Nature* **2011**, *477*, 601–605. [[CrossRef](#)]
68. Pan, X.; Li, Z.; Jin, X.; Zhao, Y.; Huang, G.; Huang, X.; Shen, Z.; Cao, Y.; Dong, M.; Lei, J.; et al. Comparative Structural Analysis of Human Nav1.1 and Nav1.5 Reveals Mutational Hotspots for Sodium Channelopathies. *Proc. Natl. Acad. Sci. USA* **2021**, *118*, e2100066118. [[CrossRef](#)]
69. Kise, Y.; Kasuya, G.; Okamoto, H.H.; Yamanouchi, D.; Kobayashi, K.; Kusakizako, T.; Nishizawa, T.; Nakajo, K.; Nureki, O. Structural Basis of Gating Modulation of Kv4 Channel Complexes. *Nature* **2021**, *599*, 158–164. [[CrossRef](#)]
70. Gao, S.; Yao, X.; Chen, J.; Huang, G.; Fan, X.; Xue, L.; Li, Z.; Wu, T.; Zheng, Y.; Huang, J.; et al. Structural Basis for Human Cav1.2 Inhibition by Multiple Drugs and the Neurotoxin Calciseptine. *Cell* **2023**, *186*, 5363–5374.e16. [[CrossRef](#)]
71. Wang, W.; MacKinnon, R. Cryo-EM Structure of the Open Human Ether-à-Go-Go-Related K<sup>+</sup> Channel hERG. *Cell* **2017**, *169*, 422–430.e10. [[CrossRef](#)]
72. Fernandes, C.A.H.; Zuniga, D.; Fagnen, C.; Kugler, V.; Scala, R.; Péhau-Arnaudet, G.; Wagner, R.; Perahia, D.; Bendahhou, S.; Vénien-Bryan, C. Cryo-Electron Microscopy Unveils Unique Structural Features of the Human Kir2.1 Channel. *Sci. Adv.* **2022**, *8*, eabq8489. [[CrossRef](#)]
73. Dong, Y.; Yu, Z.; Li, Y.; Huang, B.; Bai, Q.; Gao, Y.; Chen, Q.; Li, N.; He, L.; Zhao, Y. Structural Insight into the Allosteric Inhibition of Human Sodium-Calcium Exchanger NCX1 by XIP and SEA0400. *EMBO J.* **2024**, *43*, 14–31. [[CrossRef](#)] [[PubMed](#)]

74. Guo, Y.; Zhang, Y.; Yan, R.; Huang, B.; Ye, F.; Wu, L.; Chi, X.; Shi, Y.; Zhou, Q. Cryo-EM Structures of Recombinant Human Sodium-Potassium Pump Determined in Three Different States. *Nat. Commun.* **2022**, *13*, 3957. [[CrossRef](#)] [[PubMed](#)]
75. Beard, N.A.; Wei, L.; Dulhunty, A.F. Control of Muscle Ryanodine Receptor Calcium Release Channels by Proteins in the Sarcoplasmic Reticulum Lumen. *Clin. Exp. Pharmacol. Physiol.* **2009**, *36*, 340–345. [[CrossRef](#)] [[PubMed](#)]
76. Hadiatullah, H.; He, Z.; Yuchi, Z. Structural Insight Into Ryanodine Receptor Channelopathies. *Front. Pharmacol.* **2022**, *13*, 897494. [[CrossRef](#)]
77. Bäuerlein, F.J.B.; Renner, M.; Chami, D.E.; Lehnart, S.E.; Pastor-Pareja, J.C.; Fernández-Busnadio, R. Cryo-Electron Tomography of Large Biological Specimens Vitrified by Plunge Freezing. *bioRxiv* **2023**. [[CrossRef](#)]
78. Asghari, P.; Scriven, D.R.L.; Sanatani, S.; Gandhi, S.K.; Campbell, A.I.M.; Moore, E.D.W. Nonuniform and Variable Arrangements of Ryanodine Receptors Within Mammalian Ventricular Couplons. *Circ. Res.* **2014**, *115*, 252–262. [[CrossRef](#)]
79. Asghari, P.; Scriven, D.R.L.; Shahrasebi, S.; Valdivia, H.H.; Alsina, K.M.; Valdivia, C.R.; Navarro-Garcia, J.A.; Wehrens, X.H.T.; Moore, E.D.W. Phosphorylation of RyR2 Simultaneously Expands the Dyad and Rearranges the Tetramers. *J. Gen. Physiol.* **2024**, *156*, e202213108. [[CrossRef](#)]
80. Li, J.; Imtiaz, M.S.; Beard, N.A.; Dulhunty, A.F.; Thorne, R.; vanHelden, D.F.; Laver, D.R. SS-Adrenergic Stimulation Increases RyR2 Activity via Intracellular  $\text{Ca}^{2+}$  and  $\text{Mg}^{2+}$  Regulation. *PLoS ONE* **2013**, *8*, e58334. [[CrossRef](#)]
81. Fu, Y.; Shaw, S.A.; Naami, R.; Vuong, C.L.; Basheer, W.A.; Guo, X.; Hong, T. Isoproterenol Promotes Rapid Ryanodine Receptor Movement to Bridging Integrator 1 (BIN1)-Organized Dyads. *Circulation* **2016**, *133*, 388–397. [[CrossRef](#)]
82. Bennett, H.J.; Davenport, J.B.; Collins, R.F.; Trafford, A.W.; Pinali, C.; Kitmitto, A. Human Junctophilin-2 Undergoes a Structural Rearrangement upon Binding PtdIns(3,4,5)P3 and the S101R Mutation Identified in Hypertrophic Cardiomyopathy Obviates This Response. *Biochem. J.* **2013**, *456*, 205–217. [[CrossRef](#)]
83. Miotto, M.C.; Reiken, S.; Wronksa, A.; Yuan, Q.; Dridi, H.; Liu, Y.; Weninger, G.; Tchagou, C.; Marks, A.R. Structural Basis for Ryanodine Receptor Type 2 Leak in Heart Failure and Arrhythmogenic Disorders. *Nat. Commun.* **2024**, *15*, 8080. [[CrossRef](#)]
84. Nayak, A.R.; Rangubpit, W.; Will, A.H.; Hu, Y.; Castro-Hartmann, P.; Lobo, J.J.; Dryden, K.; Lamb, G.D.; Sompornpisut, P.; Samsó, M. Interplay between  $\text{Mg}^{2+}$  and  $\text{Ca}^{2+}$  at Multiple Sites of the Ryanodine Receptor. *Nat. Commun.* **2024**, *15*, 4115. [[CrossRef](#)]
85. Laver, D.R. Regulation of the RyR Channel Gating by  $\text{Ca}^{2+}$  and  $\text{Mg}^{2+}$ . *Biophys. Rev.* **2018**, *10*, 1087–1095. [[CrossRef](#)]
86. Laver, D.R.; Honen, B.N. Luminal  $\text{Mg}^{2+}$ , a Key Factor Controlling RYR2-Mediated  $\text{Ca}^{2+}$  Release: Cytoplasmic and Luminal Regulation Modeled in a Tetrameric Channel. *J. Gen. Physiol.* **2008**, *132*, 429–446. [[CrossRef](#)] [[PubMed](#)]
87. Sitsapesan, R.; Williams, A.J. Regulation of the Gating of the Sheep Cardiac Sarcoplasmic Reticulum  $\text{Ca}^{2+}$ -Release Channel by Luminal  $\text{Ca}^{2+}$ . *J. Membr. Biol.* **1994**, *137*, 215–226. [[CrossRef](#)] [[PubMed](#)]
88. Laver, D.R.; Roden, L.D.; Ahern, G.P.; Eager, K.R.; Junankar, P.R.; Dulhunty, A.F. Cytoplasmic  $\text{Ca}^{2+}$  Inhibits the Ryanodine Receptor from Cardiac Muscle. *J. Membr. Biol.* **1995**, *147*, 7–22. [[CrossRef](#)] [[PubMed](#)]
89. Iaparov, B.; Baglaeva, I.; Zahradník, I.; Zahradníková, A. Magnesium Ions Moderate Calcium-Induced Calcium Release in Cardiac Calcium Release Sites by Binding to Ryanodine Receptor Activation and Inhibition Sites. *Front. Physiol.* **2022**, *12*, 805956. [[CrossRef](#)]
90. Cannell, M.B.; Kong, C.H.T.; Imtiaz, M.S.; Laver, D.R. Control of Sarcoplasmic Reticulum  $\text{Ca}^{2+}$  Release by Stochastic RyR Gating within a 3D Model of the Cardiac Dyad and Importance of Induction Decay for CICR Termination. *Biophys. J.* **2013**, *104*, 2149–2159. [[CrossRef](#)]
91. Guo, W.; Sun, B.; Estillore, J.P.; Wang, R.; Chen, S.R.W. The Central Domain of Cardiac Ryanodine Receptor Governs Channel Activation, Regulation, and Stability. *J. Biol. Chem.* **2020**, *295*, 15622–15635. [[CrossRef](#)]
92. Xia, Y.; Zhang, X.; Yamaguchi, N.; Morad, M. Point Mutations in RyR2  $\text{Ca}^{2+}$ -Binding Residues of Human Cardiomyocytes Cause Cellular Remodelling of Cardiac Excitation Contraction-Coupling. *Cardiovasc. Res.* **2024**, *120*, 44–55. [[CrossRef](#)]
93. Zahradníková, A.; Pavelková, J.; Sabo, M.; Baday, S.; Zahradník, I. Structure-Based Mechanism of RyR Channel Operation by Calcium and Magnesium Ions. *PLoS Comput. Biol.* **2025**, *21*, e1012950. [[CrossRef](#)]
94. Des Georges, A.; Clarke, O.B.; Zalk, R.; Yuan, Q.; Condon, K.J.; Grassucci, R.A.; Hendrickson, W.A.; Marks, A.R.; Frank, J. Structural Basis for Gating and Activation of RyR1. *Cell* **2016**, *167*, 145–157.e17. [[CrossRef](#)] [[PubMed](#)]
95. Walweel, K.; Molenaar, P.; Imtiaz, M.S.; Denniss, A.; Dos Remedios, C.; Van Helden, D.F.; Dulhunty, A.F.; Laver, D.R.; Beard, N.A. Ryanodine Receptor Modification and Regulation by Intracellular  $\text{Ca}^{2+}$  and  $\text{Mg}^{2+}$  in Healthy and Failing Human Hearts. *J. Mol. Cell. Cardiol.* **2017**, *104*, 53–62. [[CrossRef](#)] [[PubMed](#)]
96. Walweel, K.; Laver, D.R. Mechanisms of SR Calcium Release in Healthy and Failing Human Hearts. *Biophys. Rev.* **2015**, *7*, 33–41. [[CrossRef](#)] [[PubMed](#)]
97. Laver, D.R.; Owen, V.J.; Junankar, P.R.; Taske, N.L.; Dulhunty, A.F.; Lamb, G.D. Reduced Inhibitory Effect of  $\text{Mg}^{2+}$  on Ryanodine Receptor- $\text{Ca}^{2+}$  Release Channels in Malignant Hyperthermia. *Biophys. J.* **1997**, *73*, 1913–1924. [[CrossRef](#)]
98. Laver, D.R.  $\text{Ca}^{2+}$  Stores Regulate Ryanodine Receptor  $\text{Ca}^{2+}$  Release Channels via Luminal and Cytosolic  $\text{Ca}^{2+}$  Sites. *Clin. Exp. Pharmacol. Physiol.* **2007**, *34*, 889–896. [[CrossRef](#)]

99. Kermode, H.; Williams, A.J.; Sitsapesan, R. The Interactions of ATP, ADP, and Inorganic Phosphate with the Sheep Cardiac Ryanodine Receptor. *Biophys. J.* **1998**, *74*, 1296–1304. [[CrossRef](#)]
100. Magyar, Z.É.; Bauer, J.; Bauerová-Hlinková, V.; Jóna, I.; Gaburjakova, J.; Gaburjakova, M.; Almássy, J. Eu<sup>3+</sup> Detects Two Functionally Distinct Luminal Ca<sup>2+</sup> Binding Sites in Ryanodine Receptors. *Biophys. J.* **2023**, *122*, 3516–3531. [[CrossRef](#)]
101. Gaburjakova, J.; Gaburjakova, M. Cardiac Ryanodine Receptor: Selectivity for Alkaline Earth Metal Cations Points to the EF-Hand Nature of Luminal Binding Sites. *Bioelectrochemistry* **2016**, *109*, 49–56. [[CrossRef](#)]
102. Chen, W.; Wang, R.; Chen, B.; Zhong, X.; Kong, H.; Bai, Y.; Zhou, Q.; Xie, C.; Zhang, J.; Guo, A.; et al. The Ryanodine Receptor Store Sensing Gate Controls Ca<sup>2+</sup> Waves and Ca<sup>2+</sup> Triggered Arrhythmias. *Nat. Med.* **2014**, *20*, 184–192. [[CrossRef](#)]
103. Qin, J.; Valle, G.; Nani, A.; Nori, A.; Rizzi, N.; Priori, S.G.; Volpe, P.; Fill, M. Luminal Ca<sup>2+</sup> Regulation of Single Cardiac Ryanodine Receptors: Insights Provided by Calsequestrin and Its Mutants. *J. Gen. Physiol.* **2008**, *131*, 325–334. [[CrossRef](#)] [[PubMed](#)]
104. Handhe, A.; Ormonde, C.E.; Thomas, N.L.; Bralesford, C.; Williams, A.J.; Lai, F.A.; Zissimopoulos, S. Calsequestrin Interacts Directly with the Cardiac Ryanodine Receptor Luminal Domain. *J. Cell Sci.* **2016**, *129*, 3983–3988. [[CrossRef](#)] [[PubMed](#)]
105. Goonasekera, S.A.; Beard, N.A.; Groom, L.; Kimura, T.; Lyfenko, A.D.; Rosenfeld, A.; Marty, I.; Dulhunty, A.F.; Dirksen, R.T. Triadin Binding to the C-Terminal Luminal Loop of the Ryanodine Receptor Is Important for Skeletal Muscle Excitation–Contraction Coupling. *J. Gen. Physiol.* **2007**, *130*, 365–378. [[CrossRef](#)] [[PubMed](#)]
106. Lee, J.M.; Rho, S.-H.; Shin, D.W.; Cho, C.; Park, W.J.; Eom, S.H.; Ma, J.; Kim, D.H. Negatively Charged Amino Acids within the Intraluminal Loop of Ryanodine Receptor Are Involved in the Interaction with Triadin. *J. Biol. Chem.* **2004**, *279*, 6994–7000. [[CrossRef](#)]
107. Beard, N.A.; Laver, D.R.; Dulhunty, A.F. Calsequestrin and the Calcium Release Channel of Skeletal and Cardiac Muscle. *Prog. Biophys. Mol. Biol.* **2004**, *85*, 33–69. [[CrossRef](#)]
108. Chen, H.; Valle, G.; Furlan, S.; Nani, A.; Gyorke, S.; Fill, M.; Volpe, P. Mechanism of Calsequestrin Regulation of Single Cardiac Ryanodine Receptor in Normal and Pathological Conditions. *J. Gen. Physiol.* **2013**, *142*, 127–136. [[CrossRef](#)]
109. Crotti, L.; Johnson, C.N.; Graf, E.; Ferrari, G.M.D.; Cuneo, B.F.; Ovadia, M.; Papagiannis, J.; Feldkamp, M.D.; Rathi, S.; Kunic, J.D.; et al. Calmodulin Mutations Associated with Recurrent Cardiac Arrest in Infants. *Circulation* **2013**, *127*, 1009–1017. [[CrossRef](#)]
110. Kushnir, A.; Shan, J.; Betzenhauser, M.J.; Reiken, S.; Marks, A.R. Role of CaMKII $\delta$  Phosphorylation of the Cardiac Ryanodine Receptor in the Force Frequency Relationship and Heart Failure. *Proc. Natl. Acad. Sci. USA* **2010**, *107*, 10274–10279. [[CrossRef](#)]
111. Witcher, D.R.; Kovacs, R.J.; Schulman, H.; Cefali, D.C.; Jones, L.R. Unique Phosphorylation Site on the Cardiac Ryanodine Receptor Regulates Calcium Channel Activity. *J. Biol. Chem.* **1991**, *266*, 11144–11152. [[CrossRef](#)]
112. Grimm, M.; Ling, H.; Willeford, A.; Pereira, L.; Gray, C.B.B.; Erickson, J.R.; Sarma, S.; Respress, J.L.; Wehrens, X.H.T.; Bers, D.M.; et al. CaMKII $\delta$  Mediates  $\beta$ -Adrenergic Effects on RyR2 Phosphorylation and SR Ca<sup>2+</sup> Leak and the Pathophysiological Response to Chronic  $\beta$ -Adrenergic Stimulation. *J. Mol. Cell. Cardiol.* **2015**, *85*, 282–291. [[CrossRef](#)]
113. Ji, Y.; Zhao, W.; Li, B.; Desantiago, J.; Picht, E.; Kaetzel, M.A.; Schultz, J.E.J.; Kranias, E.G.; Bers, D.M.; Dedman, J.R. Targeted Inhibition of Sarcoplasmic Reticulum CaMKII Activity Results in Alterations of Ca<sup>2+</sup> Homeostasis and Cardiac Contractility. *Am. J. Physiol. Heart Circ. Physiol.* **2006**, *290*, H599–H606. [[CrossRef](#)] [[PubMed](#)]
114. Wood, B.M.; Simon, M.; Galice, S.; Alim, C.C.; Ferrero, M.; Pinna, N.N.; Bers, D.M.; Bossuyt, J. Cardiac CaMKII Activation Promotes Rapid Translocation to Its Extra-Dyadic Targets. *J. Mol. Cell. Cardiol.* **2018**, *125*, 18–28. [[CrossRef](#)] [[PubMed](#)]
115. Erickson, J.R. Mechanisms of CaMKII Activation in the Heart. *Front. Pharmacol.* **2014**, *5*, 59. [[CrossRef](#)] [[PubMed](#)]
116. Kool, M.J.; Bodde, H.E.; Elgersma, Y.; Van Woerden, G.M. Bidirectional Changes in Excitability upon Loss of Both CAMK2A and CAMK2B. *bioRxiv* **2022**. [[CrossRef](#)]
117. Knape, M.J.; Ahuja, L.G.; Bertinetti, D.; Burghardt, N.C.G.; Zimmermann, B.; Taylor, S.S.; Herberg, F.W. Divalent Metal Ions Mg<sup>2+</sup> and Ca<sup>2+</sup> Have Distinct Effects on Protein Kinase A Activity and Regulation. *ACS Chem. Biol.* **2015**, *10*, 2303–2315. [[CrossRef](#)]
118. Uehara, A.; Murayama, T.; Yasukochi, M.; Fill, M.; Horie, M.; Okamoto, T.; Matsuura, Y.; Uehara, K.; Fujimoto, T.; Sakurai, T.; et al. Extensive Ca<sup>2+</sup> Leak through K4750Q Cardiac Ryanodine Receptors Caused by Cytosolic and Luminal Ca<sup>2+</sup> Hypersensitivity. *J. Gen. Physiol.* **2017**, *149*, 199–218. [[CrossRef](#)]
119. Wehrens, X.H.T.; Lehnart, S.E.; Reiken, S.; Vest, J.A.; Wronska, A.; Marks, A.R. Ryanodine Receptor/Calcium Release Channel PKA Phosphorylation: A Critical Mediator of Heart Failure Progression. *Proc. Natl. Acad. Sci. USA* **2006**, *103*, 511–518. [[CrossRef](#)]
120. Carter, S.; Pitt, S.J.; Colyer, J.; Sitsapesan, R. Ca<sup>2+</sup>-Dependent Phosphorylation of RyR2 Can Uncouple Channel Gating from Direct Cytosolic Ca<sup>2+</sup> Regulation. *J. Membr. Biol.* **2011**, *240*, 21–33. [[CrossRef](#)]
121. Meissner, G. The Structural Basis of Ryanodine Receptor Ion Channel Function. *J. Gen. Physiol.* **2017**, *149*, 1065–1089. [[CrossRef](#)]
122. Wei, J.; Guo, W.; Wang, R.; Paul Estillore, J.; Belke, D.; Chen, Y.-X.; Vallmitjana, A.; Benitez, R.; Hove-Madsen, L.; Chen, S.R.W. RyR2 Serine-2030 PKA Site Governs Ca<sup>2+</sup> Release Termination and Ca<sup>2+</sup> Alternans. *Circ. Res.* **2023**, *132*, e59–e77. [[CrossRef](#)]
123. Cefaratti, C.; Romani, A.M.P. Functional Characterization of Two Distinct Mg<sup>2+</sup> Extrusion Mechanisms in Cardiac Sarcolemmal Vesicles. *Mol. Cell. Biochem.* **2007**, *303*, 63–72. [[CrossRef](#)] [[PubMed](#)]

124. Miotto, M.C.; Weninger, G.; Dridi, H.; Yuan, Q.; Liu, Y.; Wronska, A.; Melville, Z.; Sittenfeld, L.; Reiken, S.; Marks, A.R. Structural Analyses of Human Ryanodine Receptor Type 2 Channels Reveal the Mechanisms for Sudden Cardiac Death and Treatment. *Sci. Adv.* **2022**, *8*, eabo1272. [[CrossRef](#)] [[PubMed](#)]
125. Titus, E.W.; Deiter, F.H.; Shi, C.; Wojciak, J.; Scheinman, M.; Jura, N.; Deo, R.C. The Structure of a Calsequestrin Filament Reveals Mechanisms of Familial Arrhythmia. *Nat. Struct. Mol. Biol.* **2020**, *27*, 1142–1151. [[CrossRef](#)] [[PubMed](#)]
126. Györke, I.; Hester, N.; Jones, L.R.; Györke, S. The Role of Calsequestrin, Triadin, and Junctin in Conferring Cardiac Ryanodine Receptor Responsiveness to Luminal Calcium. *Biophys. J.* **2004**, *86*, 2121–2128. [[CrossRef](#)]
127. Dulhunty, A.F.; Wium, E.; Li, L.; Hanna, A.D.; Mirza, S.; Talukder, S.; Ghazali, N.A.; Beard, N.A. Proteins within the Intracellular Calcium Store Determine Cardiac RyR Channel Activity and Cardiac Output. *Clin. Exp. Pharmacol. Physiol.* **2012**, *39*, 477–484. [[CrossRef](#)]
128. Park, H.; Wu, S.; Dunker, A.K.; Kang, C. Polymerization of Calsequestrin. Implications for  $\text{Ca}^{2+}$  Regulation. *J. Biol. Chem.* **2003**, *278*, 16176–16182. [[CrossRef](#)]
129. Park, H.; Park, I.Y.; Kim, E.; Youn, B.; Fields, K.; Dunker, A.K.; Kang, C. Comparing Skeletal and Cardiac Calsequestrin Structures and Their Calcium Binding: A Proposed Mechanism for Coupled Calcium Binding and Protein Polymerization. *J. Biol. Chem.* **2004**, *279*, 18026–18033. [[CrossRef](#)]
130. Marabelli, C.; Santiago, D.J.; Priori, S.G. The Structural-Functional Crosstalk of the Calsequestrin System: Insights and Pathological Implications. *Biomolecules* **2023**, *13*, 1693. [[CrossRef](#)]
131. Bal, N.C.; Jena, N.; Sopariwala, D.; Balaraju, T.; Shaikh, S.; Bal, C.; Sharon, A.; Györke, S.; Periasamy, M. Probing Cationic Selectivity of Cardiac Calsequestrin and Its CPVT Mutants. *Biochem. J.* **2011**, *435*, 391–399. [[CrossRef](#)]
132. Kilimann, M.; Heilmeyer, L.M.G. The Effect of  $\text{Mg}^{2+}$  on the  $\text{Ca}^{2+}$ -Binding Properties of Non-Activated Phosphorylase Kinase. *Eur. J. Biochem.* **1977**, *73*, 191–197. [[CrossRef](#)]
133. Ng, K.; Titus, E.W.; Lieve, K.V.; Roston, T.M.; Mazzanti, A.; Deiter, F.H.; Denjoy, I.; Ingles, J.; Till, J.; Robyns, T.; et al. An International Multicenter Evaluation of Inheritance Patterns, Arrhythmic Risks, and Underlying Mechanisms of CASQ2 - Catecholaminergic Polymorphic Ventricular Tachycardia. *Circulation* **2020**, *142*, 932–947. [[CrossRef](#)] [[PubMed](#)]
134. Bal, N.C.; Jena, N.; Chakravarty, H.; Kumar, A.; Chi, M.; Balaraju, T.; Rawale, S.V.; Rawale, J.S.; Sharon, A.; Periasamy, M. The C-Terminal Calcium-Sensitive Disordered Motifs Regulate Isoform-Specific Polymerization Characteristics of Calsequestrin. *Biopolymers* **2015**, *103*, 15–22. [[CrossRef](#)] [[PubMed](#)]
135. Beard, N.A.; Dulhunty, A.F. C-Terminal Residues of Skeletal Muscle Calsequestrin Are Essential for Calcium Binding and for Skeletal Ryanodine Receptor Inhibition. *Skelet. Muscle* **2015**, *5*, 6. [[CrossRef](#)]
136. Boncompagni, S.; Pozzer, D.; Visconti, C.; Ferreiro, A.; Zito, E. Physical and Functional Cross Talk Between Endo-Sarcoplasmic Reticulum and Mitochondria in Skeletal Muscle. *Antioxid. Redox Signal.* **2020**, *32*, 873–883. [[CrossRef](#)] [[PubMed](#)]
137. Manno, C.; Figueroa, L.C.; Gillespie, D.; Fitts, R.; Kang, C.; Franzini-Armstrong, C.; Rios, E. Calsequestrin Depolymerizes When Calcium Is Depleted in the Sarcoplasmic Reticulum of Working Muscle. *Proc. Natl. Acad. Sci. USA* **2017**, *114*, E638–E647. [[CrossRef](#)]
138. Ramay, H.R.; Fabris, F.; Noel, O.; Sarkar, A. An Il-lumen-ating Look at Ryanodine Receptor Modulation by Disruption in Triadin and Calsequestrin Interactions in Cardiac Myocytes. *J. Physiol.* **2008**, *586*, 697–699. [[CrossRef](#)]
139. Zhang, L.; Kelley, J.; Schmeisser, G.; Kobayashi, Y.M.; Jones, L.R. Complex Formation between Junctin, Triadin, Calsequestrin, and the Ryanodine Receptor. Proteins of the Cardiac Junctional Sarcoplasmic Reticulum Membrane. *J. Biol. Chem.* **1997**, *272*, 23389–23397. [[CrossRef](#)]
140. Shin, D.W.; Ma, J.; Kim, D.H. The Asp-Rich Region at the Carboxyl-Terminus of Calsequestrin Binds to  $\text{Ca}^{2+}$  and Interacts with Triadin. *FEBS Lett.* **2000**, *486*, 178–182. [[CrossRef](#)]
141. Cai, W.-F.; Pritchard, T.; Florea, S.; Lam, C.-K.; Han, P.; Zhou, X.; Yuan, Q.; Lehnart, S.E.; Allen, P.D.; Kranias, E.G. Ablation of Junctin or Triadin Is Associated with Increased Cardiac Injury Following Ischaemia/Reperfusion. *Cardiovasc. Res.* **2012**, *94*, 333–341. [[CrossRef](#)]
142. Marty, I. Triadin: A Multi-Protein Family for Which Purpose? *Cell. Mol. Life Sci.* **2004**, *61*, 1850–1853. [[CrossRef](#)]
143. Oddoux, S.; Brocard, J.; Schweitzer, A.; Szentesi, P.; Giannesini, B.; Brocard, J.; Fauré, J.; Pernet-Gallay, K.; Bendahan, D.; Lunardi, J.; et al. Triadin Deletion Induces Impaired Skeletal Muscle Function. *J. Biol. Chem.* **2009**, *284*, 34918–34929. [[CrossRef](#)] [[PubMed](#)]
144. Qin, J.; Valle, G.; Nani, A.; Chen, H.; Ramos-Franco, J.; Nori, A.; Volpe, P.; Fill, M. Ryanodine Receptor Luminal  $\text{Ca}^{2+}$  Regulation: Swapping Calsequestrin and Channel Isoforms. *Biophys. J.* **2009**, *97*, 1961–1970. [[CrossRef](#)] [[PubMed](#)]
145. Zhang, L.; Franzini-Armstrong, C.; Ramesh, V.; Jones, L.R. Structural Alterations in Cardiac Calcium Release Units Resulting from Overexpression of Junctin. *J. Mol. Cell. Cardiol.* **2001**, *33*, 233–247. [[CrossRef](#)] [[PubMed](#)]
146. Chopra, N.; Yang, T.; Asghari, P.; Moore, E.D.; Huke, S.; Akin, B.; Cattolica, R.A.; Perez, C.F.; Hlaing, T.; Knollmann-Ritschel, B.E.C.; et al. Ablation of Triadin Causes Loss of Cardiac  $\text{Ca}^{2+}$  Release Units, Impaired Excitation–Contraction Coupling, and Cardiac Arrhythmias. *Proc. Natl. Acad. Sci. USA* **2009**, *106*, 7636–7641. [[CrossRef](#)]

147. Clemens, D.J.; Ye, D.; Wang, L.; Kim, C.S.J.; Zhou, W.; Dotzler, S.M.; Tester, D.J.; Marty, I.; Knollmann, B.C.; Ackerman, M.J. Cellular and Electrophysiological Characterization of Triadin Knockout Syndrome Using Induced Pluripotent Stem Cell-Derived Cardiomyocytes. *Stem Cell Rep.* **2023**, *18*, 1075–1089. [[CrossRef](#)]
148. Manno, C.; Tammineni, E.; Figueroa, L.; Marty, I.; Ríos, E. Quantification of the Calcium Signaling Deficit in Muscles Devoid of Triadin. *PLoS ONE* **2022**, *17*, e0264146. [[CrossRef](#)]
149. di Barletta, M.R.; Viatchenko-Karpinski, S.; Nori, A.; Memmi, M.; Terentyev, D.; Turcato, F.; Valle, G.; Rizzi, N.; Napolitano, C.; Gyorke, S.; et al. Clinical Phenotype and Functional Characterization of CASQ2 Mutations Associated with Catecholaminergic Polymorphic Ventricular Tachycardia. *Circulation* **2006**, *114*, 1012–1019. [[CrossRef](#)]
150. Lodola, F.; Morone, D.; Denegri, M.; Bongianino, R.; Nakahama, H.; Rutigliano, L.; Gosetti, R.; Rizzo, G.; Vollero, A.; Buonocore, M.; et al. Adeno-Associated Virus-Mediated CASQ2 Delivery Rescues Phenotypic Alterations in a Patient-Specific Model of Recessive Catecholaminergic Polymorphic Ventricular Tachycardia. *Cell Death Dis.* **2016**, *7*, e2393. [[CrossRef](#)]
151. Kalyanasundaram, A.; Viatchenko-Karpinski, S.; Belevych, A.E.; Lacombe, V.A.; Hwang, H.S.; Knollmann, B.C.; Gyorke, S.; Periasamy, M. Functional Consequences of Stably Expressing a Mutant Calsequestrin (CASQ2D307H) in the CASQ2 Null Background. *Am. J. Physiol. Heart Circ. Physiol.* **2012**, *302*, H253–H261. [[CrossRef](#)]
152. Ayuk, J.; Gittoes, N.J.L. How Should Hypomagnesaemia Be Investigated and Treated? *Clin. Endocrinol.* **2011**, *75*, 743–746. [[CrossRef](#)]
153. Andreozzi, F.; Cuminetti, G.; Karmali, R.; Kamgang, P. Electrolyte Disorders as Triggers for Takotsubo Cardiomyopathy. *Eur. J. Case Rep. Intern. Med.* **2018**, *5*, 000760. [[CrossRef](#)]
154. Gragossian, A.; Bashir, K.; Bhutta, B.S.; Friede, R. Hypomagnesemia. In *StatPearls*; StatPearls Publishing: Treasure Island, FL, USA, 2025.
155. Fauconnier, J.; Thireau, J.; Reiken, S.; Cassan, C.; Richard, S.; Matecki, S.; Marks, A.R.; Lacampagne, A. Leaky RyR2 Trigger Ventricular Arrhythmias in Duchenne Muscular Dystrophy. *Proc. Natl. Acad. Sci. USA* **2010**, *107*, 1559–1564. [[CrossRef](#)]
156. Haigney, M.C.; Wei, S.; Käab, S.; Griffiths, E.; Berger, R.; Tunin, R.; Kass, D.; Fisher, W.G.; Silver, B.; Silverman, H. Loss of Cardiac Magnesium in Experimental Heart Failure Prolongs and Destabilizes Repolarization in Dogs. *J. Am. Coll. Cardiol.* **1998**, *31*, 701–706. [[CrossRef](#)]
157. Gusev, K.; Niggli, E. Modulation of the Local SR Ca<sup>2+</sup> Release by Intracellular Mg<sup>2+</sup> in Cardiac Myocytes. *J. Gen. Physiol.* **2008**, *132*, 721–730. [[CrossRef](#)]
158. Murphy, E.; Steenbergen, C.; Levy, L.A.; Raju, B.; London, R.E. Cytosolic Free Magnesium Levels in Ischemic Rat Heart. *J. Biol. Chem.* **1989**, *264*, 5622–5627. [[CrossRef](#)]
159. Murphy, E.; Steenbergen, C. Mechanisms Underlying Acute Protection from Cardiac Ischemia-Reperfusion Injury. *Physiol. Rev.* **2008**, *88*, 581–609. [[CrossRef](#)]

**Disclaimer/Publisher’s Note:** The statements, opinions and data contained in all publications are solely those of the individual author(s) and contributor(s) and not of MDPI and/or the editor(s). MDPI and/or the editor(s) disclaim responsibility for any injury to people or property resulting from any ideas, methods, instructions or products referred to in the content.